Robust Model Predictive Control of An Input Delayed Functional Electrical Stimulation

by

Ziyue Sun

B.S., Mechanical Engineering, University of Pittsburgh, 2015

Submitted to the Graduate Faculty of

Swanson School of Engineering in partial fulfillment

of the requirements for the degree of

Master of Science

University of Pittsburgh

2017

UNIVERSITY OF PITTSBURGH

SWANSON SCHOOL OF ENGINEERING

This thesis was presented

by

Ziyue Sun

It was defended on

September 6, 2017

and approved by

Jeffrey Vipperman, Ph.D., Professor, Vice Chair of Department of Mechanical Engineering and Materials Science and Professor, Department of Bioengineering

Zhi-Hong Mao, Ph.D., Associate Professor, Department of Electrical and Computer Engineering and Associate Professor, Department of Bioengineering

Thesis Advisor: Nitin Sharma, Ph.D., Assistant Professor, Department of Mechanical Engineering and Materials Science and Assistant Professor, Department of Bioengineering

Robust Model Predictive Control of An Input Delayed Functional Electrical Stimulation

Ziyue Sun, M.S.

University of Pittsburgh, 2017

Functional electrical stimulation (FES) is an external application of low-level currents to elicit muscle contractions that can potentially restore limb function in persons with spinal cord injury. However, FES often leads to the rapid onset of muscle fatigue, which limits performance of FES-based devices due to reduction in force generation capability. Fatigue is caused by unnatural muscle recruitment and synchronous and repetitive recruitment of muscle fibers. In this situation, overstimulation of the muscle fibers further aggravates the muscle fatigue. Therefore, a motivation exists to use optimal controls that minimize muscle stimulation while providing a desired performance. Model predictive controller (MPC) is one such optimal control method. However, the traditional MPC is dependent on exact model knowledge of the musculoskeletal dynamics and cannot handle modeling uncertainties. Motivated to address modeling uncertainties, robust MPC approach is used to control FES. Moreover, two new robust MPC techniques are studied to address electromechanical delay (EMD) during FES, which often causes performance issues and stability problems.

This thesis compares two types of robust MPCs: a Lyapunov-based MPC and a tube- based MPC for controlling knee extension elicited through FES.

Lyapunov-based MPC incorporated a contractive constraint that bounds the Lyapunov function of the MPC with a Lyapunov function that was used to derive an EMD compensation control law. The Lyapunov-based MPC was simulated to validate its performance.

In the tube-based MPC, the EMD compensation controller was chosen to be the tube that eliminated output of the nominal MPC and the output of the real system. Regulation experiments were performed for the tube-based MPC on a leg extension machine and the controller showed robust performance despite modeling uncertainties.

TABLE OF CONTENTS

LIST OF TABLES

LIST OF FIGURES

PREFACE

Acknowledgements to my research advisor, Dr. Nitin Sharma; my committee members Dr. Jeffrey Vipperman and Dr. and Zhi-Hong Mao; and Mr. Xuefeng Bao, my senior colleague in Neuromuscular Control and Robotics Laboratory.

1.0 MOTIVATIONS AND PROBLEM STATEMENT

Approximately 17,000 cases of spinal cord injury (SCI) occur each year [1]. 20% of these injuries lead to complete paraplegia. Loss of lower extremity function constricts these subjects into a wheelchair, which significantly affects their mobility and quality of life.

Functional electrical stimulation (FES), which produces involuntary muscle contractions through external application of low-level electrical current pulses has been used to restore limb movements such as hand grasp, cycling, knee extension, and walking[2]-[5]. Thus, FES holds a huge potential to restore ambulation in people with paraplegia and their integration in society [6]-[9]

One of the major challenges of FES is that it induces the muscle fatigue rapidly. Once the muscle is fatigued, the muscle produces less force than the unfatigued muscles. This limits the performance of the FES-based device. The muscle fatigue occurs because the FES synchronously and repeatedly excites muscle fibers and at a high frequency [16]. A high gain error-based feedback controller may handle muscle fatigue by increasing the amplitude or the frequency of stimulation [17][18]However, this method may result in overstimulation of muscles and cause even more muscle fatigue.

Optimal control methods can solve for the minimum amount of stimulations that is required to move the limb to a desired angle. This prevents over stimulation on muscles and thus reduce the muscle fatigue. Model predictive controller (MPC) is one such optimal control method that solves

a finite horizon optimal control problem with a priori cost function. It has been widely adopted in industry as an effective means to deal with multivariable constrained control problems. In [15], nonlinear MPC (NMPC) algorithm is used to control a nonlinear musculoskeletal knee model driven by FES. The controller solves for the optimal solution of the system with exact model knowledge. However, the MPC is not robust to the model uncertainties.

Another challenge in FES is so called electromechanical delay (EMD). The EMD is defined as the time difference between when the stimulation starts and when muscle starts to contract. It varies with time and subjects. Thus, the MPC should be able to robust to EMD.

1.1 THESIS CONTRIBUTIONS

Motivated to add on stability of the MPC despite modelling uncertainty, two robust nonlinear MPC techniques are presented and compared.

A Lyapunov based MPC technique was developed for controlling FES. The MPC control is stabilized by a Lyapunov constraint that was motivated to provide stability due to the presence of EMD in the FES-driven musculoskeletal muscle. The constraint bounds the Lyapunov function of the MPC controller with a Lyapunov function of an EMD compensating controller [53]. The EMD compensating controller is a modified proportional-derivative (PD) and dynamic surface controller (DSC) that compensates for EMD in a first-order muscle activation dynamics that is coupled to a second-order musculoskeletal dynamics. The PD+DSC technique has been proven to provide uniformly ultimately bounded stability for aforementioned dynamics. Thus, an MPC technique constrained to the Lyapunov function of the PD+DSC technique is at least guaranteed to be UUB stable. This Lyapunov-based MPC was validated through simulations.

The Lyapunov-based controller, however, does not completely address the problem of modeling uncertainties. This controller uses a nominal model for both MPC and using the Lyapunov constraint of the PD +DSC technique. Therefore, a tube-based MPC was developed that solves a finite horizon optimal control problem and uses the error between MPC predicted output and the actual plant output as a feedback. The stability of the nominal MPC was ensured by a quadratic terminal cost function with a weight found by solving an algebraic Riccati equation. Compared to the Lyapunov-based MPC, the method has significantly reduced computation time. Therefore, in addition to simulations, the tube-based MPC was validated through experiments.

2.0 BACKGROUND AND INTRODUCTION

2.1 REVIEW OF FUNCTIONAL ELECTRICAL STIMULATION

Functional electrical stimulation applies short electrical pulses to motor neurons to generate muscle contractions with the aim to generate limb movements that mimic the voluntary movements. The electric current of stimulation is transduced to muscle tissues through external electrodes. There are three types of electrode placements: surface electrode (the electrodes are attached to the skin surface), percutaneous electrodes (the electrodes that are placed within the muscle body) and the implanted electrodes (the electrodes are attached to muscle nerve) [49]. The tension produced in stimulated muscle depends on the pulse amplitude, duration, frequency and as well as the pulse shape of the stimulation. In most neural prosthesis, the strength of muscle contraction is controlled by modulating the amplitude and//or pulse duration. The stimulus frequency is usually set to be constant and low in the range of 30-40 Hz to postpone the fatigue.

Numerous applications on FES have been established for reconstructing functional movements such as hand grasp, cycling, knee extension, etc. In [2], an implanted neuroprosthetic system with FES for grasping muscles of one arm was designed. 51 tetraplegic adults with C5 or C6 level injuries participated in the research and 49 of them had improvement in grasp-release abilities. In [3], team Hasomed developed a training technique for FES cycling for SCI subjects. In [5], a hybrid controller of FES and electric motor was designed to produce a knee extension.

Regularly FES training can make the muscle fibers attain strength and thus, gradually restore muscle functions [11]. And therefore, it is useful for improving the patients' activities of daily living. However, due to the nature of FES stimulation, muscle fibers are recruited synchronously at frequencies higher than physiological frequency. [12]. Thus, muscles fatigue rapidly and is a major safety concern, particularly for lower-limb activities due to the risk of falls and possible injury. Once the muscle is fatigued, the parametric changes occur, for example, force-length relationship is affected [13] This can lead to loss in control effectiveness and hence inability to produce limb movements. High gain error-based feedback controllers are usually used to compensate the fatigue that increase stimulation amplitude or stimulation frequency on the onset of muscle fatigue [17][18]. However, these high gain feedback methods can overstimulate the muscles, which further aggravates muscle fatigue. Recently hybrid neuroprosthesis have been proposed that use an electric motor to compensate for muscle fatigue by load sharing or provide full assistance in case of loss in control effectiveness [5][19].

The work in this thesis is motivated to minimize or to delay the onset of muscle fatigue by using a model predictive control method that solves for stimulation inputs that minimizes a priori cost function. The MPC optimizes stimulation inputs while obtaining desired error performance, keep stimulation within prescribed limits, and thus avoids overstimulation. Recently, nonlinear MPC has been experimentally validated in FES applications. In [22], a nonlinear MPC was developed for paraplegic standing up. In [15], a nonlinear MPC was designed to compute the minimum amount of stimulation necessary to produce a desired motion.

2.2 REVIEW OF MODEL PREDICTIVE CONTROL

Model Predictive Control (MPC), also referred to as Receding Horizon Control and Moving Horizon Optimal Control, is a widely used optimal control technique that searches for the optimal solution in a feasible set [26]. The concept structure of MPC is illustrated in Figure 1.

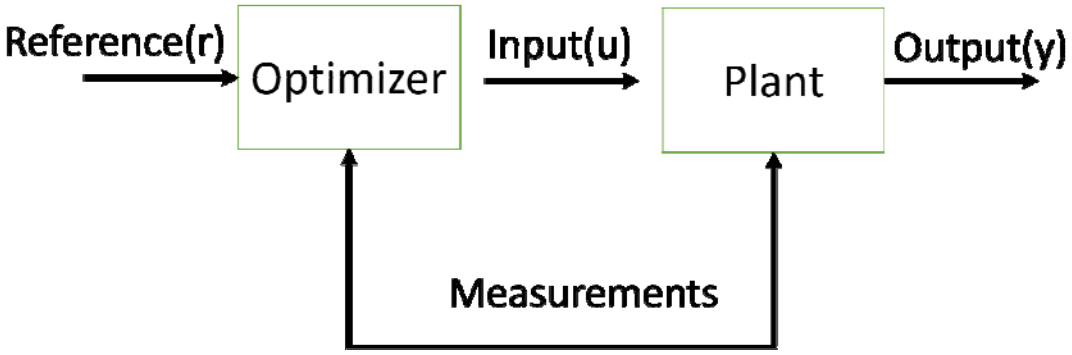

Figure 1 MPC block diagram

In the MPC method, a plant is controlled by predicting future output behavior based on a nominal model of the plant. A cost function composed of tracking error and control input is minimized over a finite time horizon. A finite set of optimal control inputs are predicted over a pre-defined horizon. Once the finite horizon optimization problem is solved, only the first solved control input value is implemented, and the rest of the trajectory is discarded; this optimization procedure is then repeated in every future sampling step. The first manipulated input value is then set to be the initial guess of the next step. This is the so-called receding horizon scheme. Figure 2 illustrates the MPC scheme, the relationship between the predicted output and reference output, the past control input and the predicted control input. It shows the inputs and outputs within and out of the prediction horizon and shows how the prediction horizon moves with time.

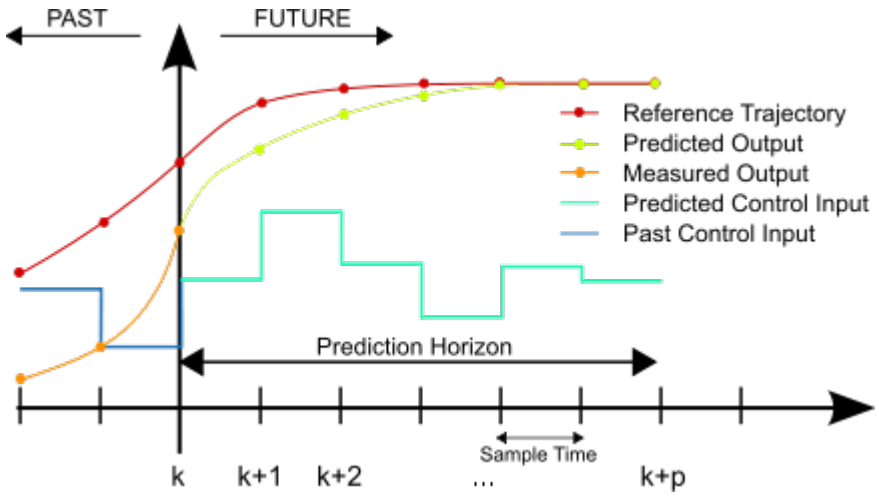

Figure 2 MPC scheme from [27]. This shows the input and output in the prediction horizon

There are three most important issues that need to be discussed for an MPC method, feasibility, stability and robustness. The stability of conventional MPC system is usually imposed by two methods: a terminal state constraint and a terminal state cost [28]-[31]. When terminal state constraints are used, the MPC problem may become infeasible if the terminal constraints and input constraints contradict. The stability when imposed by terminal cost method selects a weight of terminal cost function by solving an algebraic Riccati equation [28], but for nonlinear system this way of selecting terminal cost can only approximately satisfy the stability condition [30]. Still, the performance of MPC depends on the exactness of the nominal model. If the difference between the model and the real plant, or the model uncertainty is too high, it can cause the control performance to be unsatisfactory and system instability. So, the robustness is the third important issue for an MPC. If the model uncertainty is high and noise exists, the stability property cannot be guaranteed.

MPC techniques that explicitly consider the model uncertainties are called robust model predictive controller (RMPC). Many RMPC methods have been developed in the past two decades.

Min-max MPC is one of the most commonly used method to solve the robustness problem. It was first proposed by Campo and Morari [33]. The strategy is to minimize the cost function for the worst possible case of the uncertainty. The advantages of min-max MPC are that it can be applied to the output tracking and the regulation problem with disturbances and it can improve the robustness within the stability region. However, the computational burden is heavy, and it is hard to implement on a real time closed-loop controller. Another two important robust MPC methods that have been recently developed are: tube-based MPC and Lyapunov-based MPC, which will be discussed in more detail in the following sections.

2.3 REVIEW OF LYAPUNOV-BASED MPC

Lyapunov-based MPC (Lyapunov-based MPC) was recently developed, which allowed for an explicit characterization of the stability and controller feasibility and closed-loop stability. In Lyapunov-based MPC, a contractive constraint, also known as a Lyapunov constraint, is used to bound the Lyapunov function of the MPC nominal model, where the contractive constraint is obtained by applying an input trajectory under an intrinsic stabilizing law, defined as Lyapunov control, to the nominal system. In this sense, Lyapunov-based MPC method can characterize the stability region of a closed-loop system with a set of feasible initial inputs because the Lyapunov function of the nominal model is bounded with a feasible Lyapunov constraint [35][36], and the optimal solution is searched in a stability set, therefore MPC stability is satisfied automatically. In practice, the input trajectory under Lyapunov control law is used as the initial guess for the optimization in MPC so that the feasibility is ensured. If the stabilizing law is robust to the system parameter estimation error and communication flaw, MPC can also be stabilized even with an

imperfect nominal model. Lyapunov-based MPC is also considered to reduce computational complexity and improve the robustness of the control performance of optimization problem [36].

In [37], a contractive constraint was added to MPC, which restricted the Lyapunov function of the system to decrease over the prediction horizon while allowing it to increase only when the horizon was being switched. In [38][39][40] an auxiliary Lyapunov-based analytical bounded control was designed for systems with soft state constraints. In [41] a type of terminal region and cost via utilizing the hybrid of Lyapunov-Krasovskii and Lyapunov-Razumikhin condition (like Lyapunov-based MPC) was designed to stabilize a nonlinear system with known constant time delay. There is also a significant amount of research on the application of Lyapunov-based MPC on stabilizing the nonlinear system with communication flaws, like mode switch [38], data loss [42], asynchronous measurements [43], and time-varying measurement delays [23]. A universal construction of feedback control law based on the Lyapunov function of system [50] was adopted in those works and stability can be proven in the presence of communication flaws in states with proper assumptions. [42][43] assume the existence of a control Lyapunov function (CLF) for the system to make Lyapunov-based MPC and the value of the Lyapunov function is bounded on compact sets.

However, the Lyapunov-based MPC has not been applied to a system with input time delay. Besides, the previous Lyapunov-based MPC methods require a Lyapunov controller that makes the system asymptotically stable. While for the leg extension system or even more complicated neuromuscular dynamics, the input delay caused by electromechanical delay (EMD) is unavoidable and the controller with asymptotical stability is hard to find. Thus, an Lyapunov-based MPC which can compensate for the input delay and does not need asymptotical stability assumptions is necessary and meaningful.

2.4 REVIEW OF TUBE-BASED MPC

The first complete tube-based MPC was developed by DQ Maynne in 2006 [44]. In this paper, he developed MPC for a constrained linear system with state and measurement uncertainties. The basic idea of this kind of controller is to set up a tube, the center of which is obtained by solving the disturbance-free model predictive problem. Then the real system output can be bounded by the tube, within the range of a pre-computed invariant set. The stability and feasibility can be ensured, and robustness is increased by the diameter of the tube [44][45]. Figure 3 shows how the ultimate output is bounded by a tube. This controller reduces the computational complexity by using a Luenberger observer and can be implemented as simple as a nominal model predictive controller can be implemented.

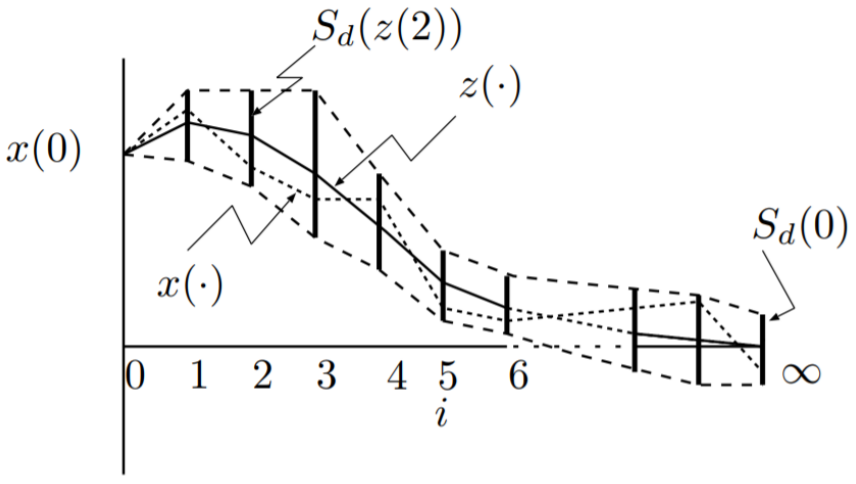

Figure 3 The output of tube-based MPC is bounded by an invariant set, from [31]. In this figure, *x* denotes the real system output, *z* denotes the nominal MPC output, S_d denotes the level set, in which the cost function defined by the error of *x* and *z* can be bounded for all *z*.

This model predictive controller can also be extended to a constrained nonlinear system [45]. Additional model predictive controller was designed as the ancillary controller to minimize the deviation between the output of nominal model and real system. Two optimal control problems were solved at the same time. One solved a standard nominal model and the other solved the ancillary problem, the solution of which drove the states towards the nominal trajectory and therefore kept the real trajectory in a tube centered by the nominal trajectory. In [46], a tube-based MPC was applied to a continuous-time plant model. A piecewise constant term was computed as the solution of an MPC problem for the nominal system to simplify the computation, and a continuous-time linear feedback law was fed by the difference between the true and nominal state trajectories.

In this thesis, the tube-based MPC is used by combining a nominal MPC and a feedback controller, where the feedback controller replaces the outer MPC and the tube is specifically designed for shrinking the error caused by EMD as well as other disturbances such as parameter estimation errors.

2.5 ROBUST MPC (RMPC) FOR INPUT DELAYED FES

In this thesis, tube-based MPC and Lyapunov-based nonlinear MPC are applied to control FES of a quadriceps muscle. Only quadriceps muscle group is stimulated which produces knee extension and gravity drives the shank back to the equilibrium position. These robust MPC methods are motivated by the need to overcome modeling uncertainties and electromechanical delay in the input. Modeling uncertainties is a big challenge due to inter-person differences and day-to-day variations in the model. The EMD is defined as the time from when the muscle is stimulated to

when the muscle starts to contract. This delay causes a lag in muscle activation and is modeled as an input delay in the musculoskeletal dynamics driven by FES. The EMD can be time-varying and be different among person to person. [47] found that the EMD could be varying with the stimulus intensity which changed in the control process and [48] brought up the idea that Neuromuscular training caused a decrease in EMD.

Some research has observed the EMD issue and made compensations in their control designs [51][52][53] but muscle fatigue issue was beyond the contents. The work in [53] developed a PD-type dynamic surface controller (DSC) to deal with a musculoskeletal system with activation dynamics and an input delay. The controller is also robust to the model parameter estimation error. The PD-type DSC feedback technique is used for the tube-based MPC method. The tube is centered by the conventional MPC for the nominal model with a known constant input time delay. The feedback control law of DSC bounds the error between the nominal output and real system output in invariant set, which composites the cross section of the tube. A DSC controller is designed to minimize the deviation between the nominal output trajectory and the output of the input delayed real plant. The DSC controller aims to move the real output to a target output which is the output of nominal MPC. This method at least assures uniform ultimately bounded stability.

For the Lyapunov-based MPC method, the Lyapunov function of the PD-type DSC technique [53] is used to form the contractive constraint. This ensures stability and feasibility of the MPC method. The PD-type DSC feedback was shown to be uniformly ultimately bounded (UUB) [53]. Thus, the Lyapunov-based MPC can solve for the optimal input by further reducing the cost under the feasible region defined by the Lyapunov constraint. A simulation is performed on a leg extension system and the results demonstrate feasible performance of this control method.

3.0 DYNAMICS FORMULATION

The FES-driven musculoskeletal dynamics of the shank, as shown in Figure 4, can be expressed [53] as

$$J\ddot{q}(t) + M_p(\dot{q}, q) + M_g(q) + w(t) = \tau_{ke}, \tag{3.1}$$

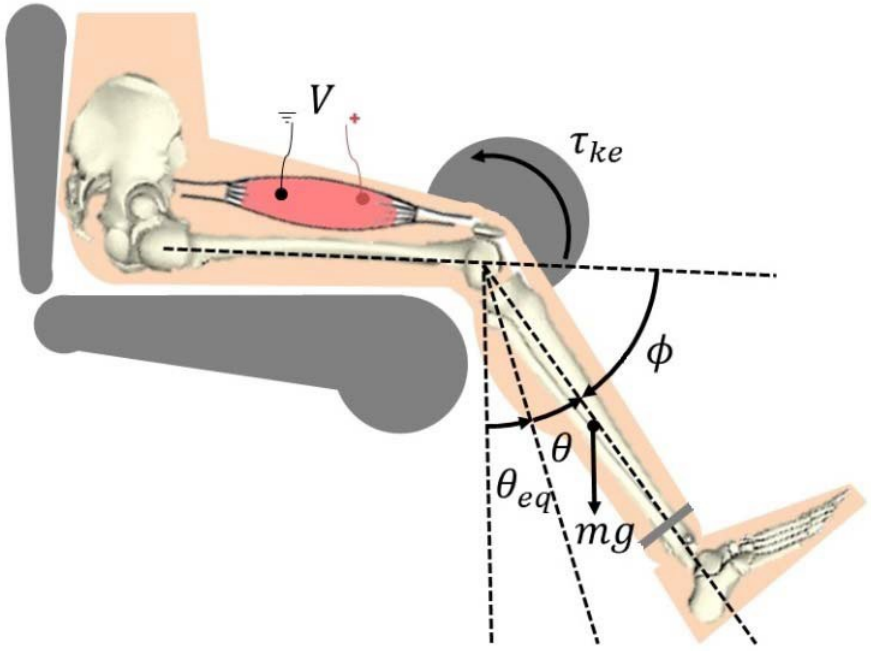

Figure 4 Leg extension model, where Φ is the control angle, θeq represents for the natural position of the shank, V is the stimulation input and τ_{ke} is the torque caused by electrical stimulation

where $J \in \mathbb{R}$ is the known constant inertia of the shank. $M_p(\dot{q}, q) \in \mathbb{R}$ is the moment generated by the passive viscous and elastic properties of the muscles,

$$M_p = d_1(q - q_0) + d_2\dot{q} + d_3 e^{d_4 q} - d_5 e^{d_6 q}, \tag{3.2}$$

and $M_g \in \mathbb{R}$ is the gravitational torque, where d_i (i =1,2,3,4,5,6) are subject parameters.

$$M_g = mgl\cos(q). \tag{3.3}$$

where *mg* is the gravitational force of the shank and *l* is the length of the shank. $w \in \mathbb{R}$ denotes the disturbance of the real system. The knee torque, τ_{ke} is defined as

$$\tau_{ke} = \varsigma(q)\eta(q, \dot{q})a_{ke} \tag{3.4}$$

where a_{ke} represents the dynamics of the actuation and is governed by

$$\dot{a}_{ke} = \frac{u(t-\tau) - a_{ke}}{T_a}, \tag{3.5}$$

$\varsigma \in \mathbb{R}$ denotes a positive moment arm that changes with respect to the joint angle, and $\eta \in \mathbb{R}$ denotes the nonlinear function of the muscle force-length and force-velocity relationships. $u \in [0,1]$ is the normalized electrical stimulation amplitude which has a time delay caused by electromechanical delay (EMD). And $T_a \in \mathbb{R}$ is the muscle activation time constant. To simplify the derivations, $u(t-\tau)$ is denoted by u_τ, and $\Omega \in \mathbb{R}$ is introduced and is defined as $\Omega = \varsigma\eta$, where

$$\Omega = (c_2\phi^2 + c_1\phi + c_0)(1 + c_3\dot{\phi}) \tag{3.6}$$

where $c_i[i = 0,1,2,3]$ are subject parameters and vary by subjects.

The dynamics of the system can be expressed as

$$\dot{x}(t) = f(x(t), u(t-\tau), w), \tag{3.7}$$

The dynamics in a state space form can be expressed as

$$\dot{x} \quad = \quad k(x) + g(x)u(t-\tau) + d(t), \tag{3.8}$$

where

$$x = \left[x_1, x_2, x_3\right]^T = \left[q, \dot{q}, a_{ke}\right]^T,$$

$$k(x) = \begin{bmatrix} x_2 \\ \Psi(x) \\ \dfrac{-x_3}{T_a} \end{bmatrix}, \qquad g(x) = \begin{bmatrix} 0 \\ \dfrac{1}{J} \\ \dfrac{1}{T_a} \end{bmatrix}, \quad d = \begin{bmatrix} 0 \\ w \\ 0 \end{bmatrix} \tag{3.9}$$

$$\Psi(x) = \frac{1}{J}(-M_v - M_e - M_g + \Omega x_3),$$

To facilitate the control development and stability analysis, the following assumptions are made:

Assumption 3.1: The inertia $J(\phi)$ is positive and is bounded by known constants $\bar{J}$ (i.e. $\left|J\right| \le \bar{J}$).

Assumption 3.2: $f(\cdot) \in \mathbb{R}^3$ is a bounded locally Lipschitz vector function, and system possesses a stable equilibrium at the origin.

Assumption 3.3: The nonlinear disturbance term i.e., $w(t)$, more specifically, $w(t) \in \mathcal{W}$, where $\mathcal{W} := \{w \in \mathbb{R} \mid \left\|w\right\| \le \varpi, \varpi > 0\}$; and its first-time derivatives are bounded, $\dot{w}(t) \in \mathcal{L}_\infty$.

Assumption 3.4: The desired trajectory $x_d(t)$, which includes the desired angular position $q_d \in \mathbb{R}$ and desired angular velocity $\dot{q}_d \in \mathbb{R}$, is designed such that $x_d(t)$, $x_d^{(i)}(t) \in \mathcal{L}_\infty$, where $x_d^{(i)}(t)$ denotes the i^{th} time derivative for $i = 1, 2, 3, \ldots$; and if $x(t)$, $\dot{x}(t) \in \mathcal{L}_\infty$, then $J(q)$, τ_p and their first time derivatives exist and are bounded.

Assumption 3.5: There exists a control law $h \in \mathbb{R}$ that drives the system (3.7) stable with constraints on input, i.e., control law h ensures the Lyapunov function of nominal system to be bounded.

4.0 CONTROL DEVELOPMENT

4.1 LYAPUNOV BASED MPC

4.1.1 MPC Formulation

In this section, we introduce the Lyapunov-based MPC design which explicitly characterizes the stability region and guarantees controller feasibility and closed-loop stability. The formulation of the Lyapunov-based MPC is as follows:

The nominal system dynamics can be expressed as

$$\dot{\bar{x}}(t) = f(\bar{x}(t), u(t-\tau), 0). \tag{4.1}$$

For the predictive control of the system of (3.7) the Lyapunov-based MPC is designed based on an existing explicit control law $h(x)$ which is able to stabilize the closed-loop system and satisfies the conditions of Equations (3.2)-(3.6).

The optimal control problem can be formulated as follows:

$$\min_{u(t)} C(\bar{x}, u) = \int_{t_0}^{t_0+T} l(\bar{x}(t), u(t))dt \tag{4.2}$$

$$\text{subject to: } \dot{\bar{x}}(t) = f(\bar{x}(t), u(t-\tau)) \tag{4.3}$$

$$\dot{\hat{x}}(t) = f(\hat{x}(t), h(\hat{x}(t))) \tag{4.4}$$

$$\bar{x}(t_0) = \hat{x}(t_0) = x(t_0) = x_0 \tag{4.5}$$

$$h \in \mathcal{H}, u \in \mathcal{U}, \mathcal{H} \subseteq \mathcal{U} \tag{4.6}$$

$$V(\bar{x}(t)) \leq V(\hat{x}(t)) \tag{4.7}$$

The dynamics (4.3) is defined in (4.1), and (4.4) is the nominal system which is driven by Lyapunov control h, where $\hat{x} = [\hat{q}, \dot{\hat{q}}, \hat{a}_{ke}]^T$, are the joint angular position, velocity, muscle activation and muscle fatigue of the nominal model; $V(\bar{x}(t))$, which is PD, is the Lyapunov function of the nominal system (4.3); $V(\hat{x}(t))$, which is PD, is the Lyapunov function of the system (3.7) driven by h.

The optimization problem is to solve optimal input trajectory $u(t)$ over the time horizon $[t_0, t_0 + T]$ by minimizing the cost function $J(x,u) \in \mathbb{R}^+$ while satisfying the constraints. The integral performance index, $l(x,u) \in \mathbb{R}^+$, can be defined as:

$$l(x(t), u(t)) = \Delta x^T(t) Q \Delta x(t) + \Delta u^T(t) R \Delta u(t),$$

where $\Delta x(t) = x_d(t) - x(t)$, $\Delta u(t) = u_d(t) - u(t)$, $x_d(t) \in \mathbb{R}^{3\times 1}$ are the desired states at time t, which were stated before, and $u_d(t) = u_{ke} \in [0,1]$ is the desired control inputs at time t. The weight matrices $Q \in \mathbb{R}^{3\times 3}$, $R \in \mathbb{R}$ are positive definite (PD).

Property 4.1: There must exist at least one feasible input trajectory u that enables all the constraints to be satisfied if the initial state is in the stability region. The control law h is defined so that the Lyapunov function of the nominal model, $V(\hat{x}(t))$ is at least bounded. For the system (4.3) and (4.4),their initial conditions are identical, meanwhile the initial states are starting from the stability region, therefore, if u is identical to h then all constraints are satisfied. It is

reasonable to have the worst scenario that cannot find a smaller Lyapunov function $V(\bar{x}(t))$ then the optimal states are $\hat{x}$ and the input trajectory u could exactly equal the control law h. So that constraint (4.3)-(4.7) are always satisfied. Usually, the feasible set is a $n+1$ dimensional tube along time axis, which contains the curve presenting control h, in this case control allocation can be evaluated by MPC to get the optimal trajectory.

4.1.2 Lyapunov Controller

The Lyapunov controller provides a feedback control law which ensures the stability of the control system and the initial feasibility of the MPC.

The Lyapunov function of the nominal system under Lyapunov control law can be defined as:

$$V_{LK} \triangleq \frac{1}{2}\hat{e}_1^2 + \frac{1}{2}\hat{e}_2^2 + \frac{1}{2}\hat{e}_{3dc}^2 + \frac{1}{2}\hat{e}_3^2 + P. \tag{4.8}$$

Error of the nominal position under Lyapunov control from the desired position, $\hat{e}_1(t) \in \mathbb{R}$, is defined as $\hat{e}_1(t) = q_d - \hat{q}$. The auxiliary error signal $\hat{e}_2(t) \in \mathbb{R}$ is defined as $\hat{e}_2 = \dot{\hat{e}}_1 + \alpha_1 \hat{e}_1$, $\hat{q}$ is the angular position. $e_{3dc} \in \mathbb{R}$ and $e_3 \in \mathbb{R}$ are defined as

$$\hat{e}_{3dc} = x_{3f} - \hat{x}_3 - e_I, \hat{e}_3 = x_{3d} - x_{3f},$$

with actual muscle activation signal $\hat{x}_3(t)$, desired signal $x_{3d}(t) = ke_2$, filtered desired signal $x_{3f}(t)$, which satisfies $\tau_3 \dot{x}_{3f} + x_{3f} = x_{3d}$ and a delay compensation term $e_I = \int_{t-\tau}^{t} u(\theta) d\theta$. $P \in \mathbb{R}^+$ is Lyapunov Krasovskii (LK) functionals,

$$P = \omega \int_{t-\tau}^{t} \left(\int_{s}^{t} \left\| \dot{u}(\theta) \right\|^2 d\theta \right) ds,$$

where $\omega \in \mathbb{R}^+$ is a subsequently defined control gain. Lyapunov function (4.8) is defined to be PD and satisfies the following inequality:

$$\lambda_1 \left\| y \right\|^2 \leq V_{LK} \leq \lambda_2 \left\| y \right\|^2$$

where $\lambda_1, \lambda_2 \in \mathbb{R}^+$, $y(t) \in \mathcal{D} \subset \mathbb{R}^5$

$$y \triangleq \left[\hat{e}_1 \quad \hat{e}_2 \quad \hat{e}_{3dc} \quad \hat{e}_3 \sqrt{P} \right]^T,$$

Proposition 4.1: With a Lyapunov control law designed as

$$u = h(t) = \alpha_2 \hat{e}_{3dc} + \dot{x}_{3f}$$

The system is semi-globally uniformly ultimately bounded (SGUUB) if the control gain k, α_1, α_2 satisfy some certain conditions [53].

$$\begin{aligned} & k_1 > 1, \quad \alpha_1 > 0, \quad \frac{1}{\tau_3} \geq \frac{1}{\kappa} \left[\frac{1}{2} + \frac{M^2}{2\varepsilon} + k_o \right] \\ & \alpha_2 \geq max \left\{ \frac{1}{2} \left(\sqrt{\nu^2 + 4\tau\tau_3} + \nu \right), \ \frac{1}{2} \left(\sqrt{\tau^2 + 4\tau} + \tau \right) \right\} \end{aligned} \tag{4.9}$$

τ is the EMD, k_o and ε are arbitrary constants. M is the maximum of x_{3d}, $\nu = \frac{1}{2} + \frac{T_a^2}{2\varepsilon} + \tau\tau_3$ and $\kappa = 1 - \tau\alpha_2^{-1} - \tau\alpha_2^{-2}$.

Proposition 4.2: The control law is sufficient to make the Lyapunov function of the nominal system UUB with satisfying the gains conditions in (4.9).

$$V(y,t) \le V(0)e^{-\frac{\delta}{\lambda_2}t} + \frac{\nu\lambda_2}{\delta}\left(1 - e^{-\frac{\delta}{\lambda_2}t}\right).$$

$\delta \in \mathbb{R}^+$ is constant lower bound of $\bar{\psi}$.

$$\bar{\psi} = min\left\{\left(\psi - \frac{\rho(\| z \|)^2}{4k_2}\right), \left(\beta - \frac{\tau\zeta_3}{\beta} - \nu\right), k_o, \frac{1}{2\tau}\right\}.$$

For full proof please read [53].

4.1.3 Stability Analysis

Corollary 4.1: Combining property 4.1 and proposition 4.1, 4.2, it can be summarized that there must exist a continuous control trajectory $u(t)$ that ensures actual system to be at least UUB while minimizing the cost function and satisfying all constraints.

In fact, if the constraint (4.7) is replaced by $V(\bar{x}(t)) \le \delta$ ($\delta \in \mathbb{R}^+$), or $\dot{V}(\bar{x}(t)) \le 0$, the MPC nominal system can be bounded as well, but it does not guarantee the constraint (4.6) holds, i.e., it may break the condition as requesting the solutions to be outside of the feasible region. According to Property 4.1, if V_{LK} is used to replace δ, at least one feasible solution exists, which is the control h. As each term in (4.8) is PD, so the truncated function is also PD, e.g.

$$V_r(\hat{x}(t)) = \frac{1}{2}\hat{e}_1^T\hat{e}_1 + \frac{1}{2}\hat{e}_2^T\hat{e}_2 + \frac{1}{2}\hat{e}_{3dc}^2 + \frac{1}{2}\hat{e}_3^2 \ . \tag{4.10}$$

The Lyapunov function of the MPC nominal system can be defined as:

$$V(\bar{x}(t)) = \frac{1}{2}\bar{e}_1^T\bar{e}_1 + \frac{1}{2}\bar{e}_2^T\bar{e}_2, \tag{4.11}$$

where $\bar{e}_1 = (q_d - \bar{q})$. and $\bar{e}_2 = \dot{\bar{e}}_1 + \alpha_1 \bar{e}_1$ This Lyapunov function can save some calculations.

Replacing (4.7) with $V(\bar{x}(t)) \leq V_r(\hat{x}(t))$, there exists a continuous control trajectory $u(t)$ ensures actual system to be at least UUB while satisfying all constraints and minimizing the cost function.

Because the Lyapunov-based MPC model does not consider the disturbance of the system, the stability of MPC with disturbance has not been proved, so it is not reliable for an experiment on a real subject. Plus, the Lyapunov constraint includes the Lyapunov function at each time step during the prediction horizon, which means the Lyapunov function values must be calculated at every iteration and this could be a huge burden, again it increases the difficulty of applying it into real experiments. So, it is of vital important to develop a new type of MPC which can deal with the model disturbance as well as the computational load. That is the main reason of developing tube-based MPC.

4.1.4 Simulation results

The optimal solution of optimal control problem in (4.2) was searched via interior point method. Firstly, the starting point, i.e., initial guess, was selected to be the control *h*; then the barrier function was constructed to release the constraints; Finally, the solution was solved by proper numerical methods. The estimated parameters of the model are listed in Table 1.

Table 1 Estimated parameters of subject A2

Parameter	Value	Parameter	Value
α	$3.64\frac{1}{kgm^2}$	d_6	-15.4
β	$64.14\frac{1}{kgm^2}$	c_0	56.9 Nm
θ_{eq}	0.35 radians	c_1	39.8 Nm
d_1	8.28 Nm	c_2	-28.9 Nm
d_2	2.46 Nms	c_3	1.2
d_3	2.29×10^{-14} Nm	T_a	0.14 seconds
d_4	18.1	I_t	35 mA
d_5	10.6 Nm	I_s	80 mA

The gains or constants in PD-DSC controller are α_1=10.48, α_2=6.14, k=10.1, $\tau_3 = 0.018$. Prediction time horizon of Lyapunov-based MPC was set to be 0.6 seconds and the input time delay value to be 80ms, simulations were run through a one degree of freedom leg extension system. The diagonal weigh matrices are:

$$diag(Q) = [100, 5, 1];$$
$$R = 10$$

After adding a 100ms input time delay to make the mismatch between the model and the system, results can be shown in the following figures.

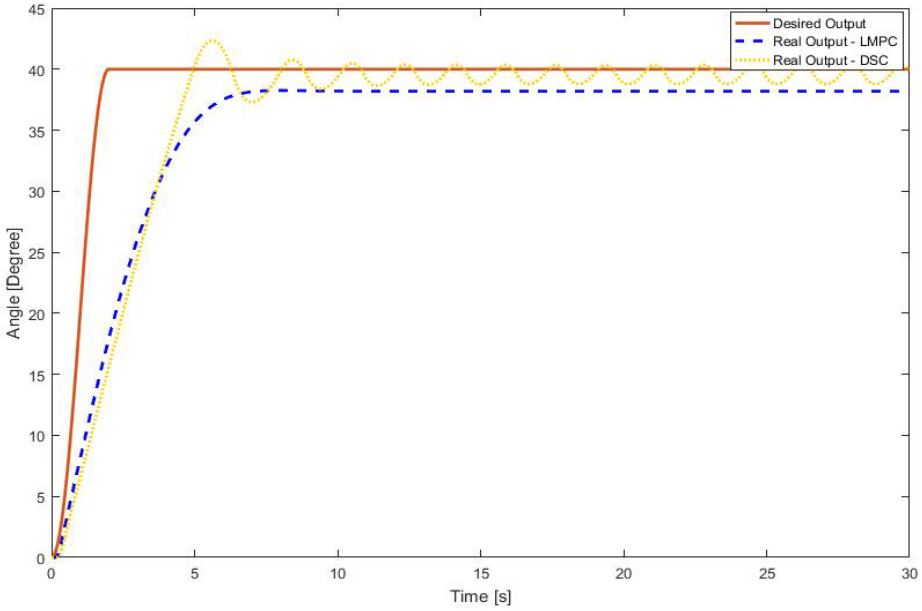

Figure 5 Output performance of the DSC (solid yellow) and Lyapunov-based MPC (dashed blue). Desired output is in red

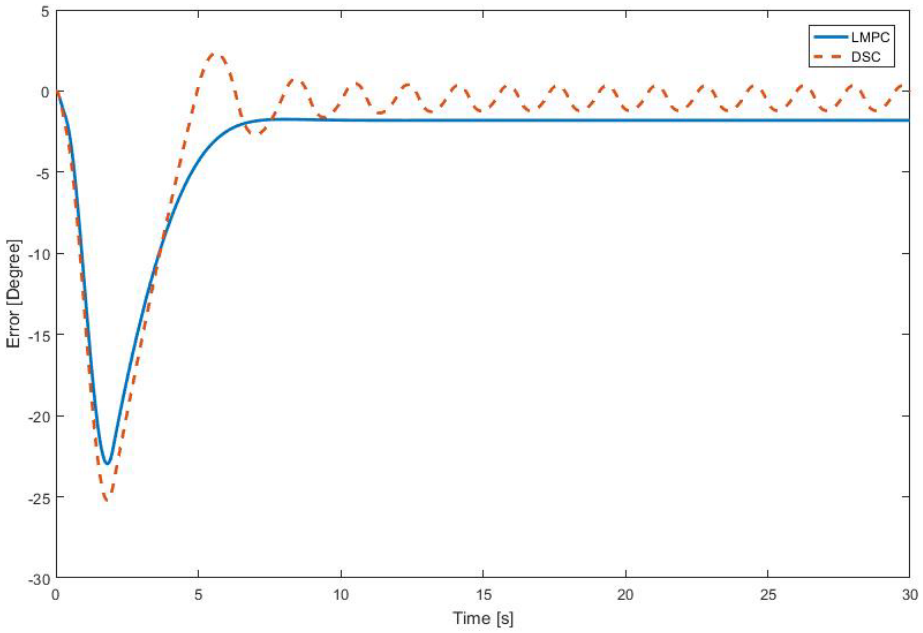

Figure 6 Output error of DSC (dashed red) and Lyapunov-based MPC (solid blue)

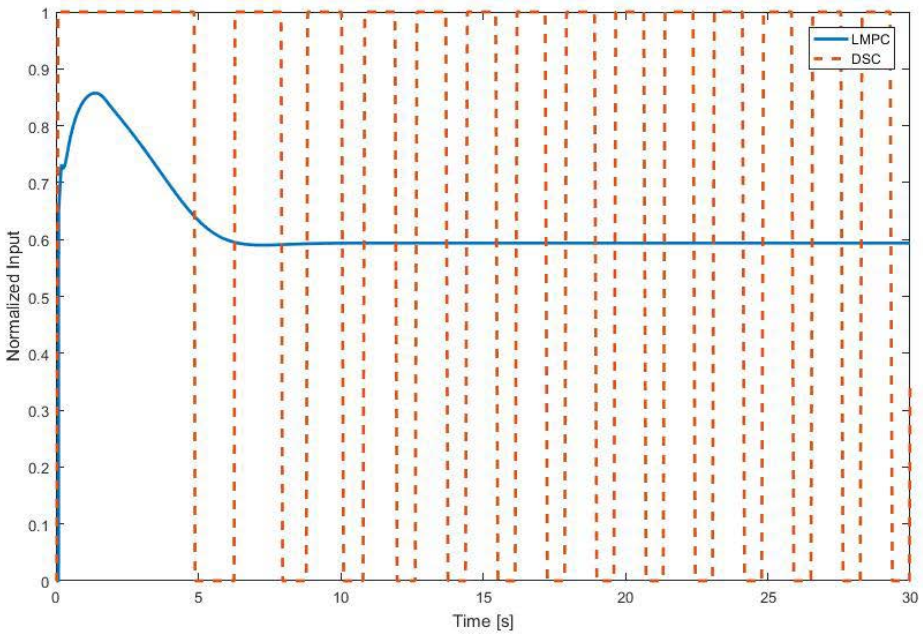

Figure 7 Normalized FES input of DSC (dashed red) and Lyapunov-based MPC (solid blue)

Simulation results indicate the performance of this control. PID-DSC controller is the Lyapunov controller and be proved to make the system stable and the Lyapunov-based MPC can stabilize the system because of the Lyapunov constraint. From Figure 5, both two of the controllers can obtain the input to stabilize the system but it is obvious that the Lyapunov-based MPC makes the output behavior smoothier and does not cause overshoot and oscillation. This is because the Lyapunov-based MPC uses the result of DSC and updates this input to optimize the solution. By calculating the RMS error of the two controllers, $Err_{RMS,PD\text{-}DSC}$ =6.04 (degrees), $Err_{RMS,LMPC}$ =5.76 (degrees), we can find the decreasing in error for Lyapunov-based MPC controller. From Figure 6 we could see that the angular position error under Lyapunov-based MPC is expected to be lower than the error under control *h*. By comparing the inputs of two controllers from Figure 7,

Lyapunov-based MPC tends to decrease the oscillation and saturation. The total input value changes can be obtained by calculating the RMS value, where $Urms_{,PD\text{-}DSC}$ =0.8 and $Urms_{,LMPC}$ =0.62. The total cost composed by tracking error and input torque of Lyapunov-based MPC is less than the DSC controller which matches our initial guess. Above all, Lyapunov-based MPC can solve for a set of inputs which tend to minimize the cost and can stabilize the states of the system.

4.2 TUBE-BASED MPC

The tube-based MPC can be treated in two parts. The first part is a nominal MPC, where the uncertainties and disturbances are not included, i.e., the nominal model is assumed to be the same as the plant. This MPC solves the cost function that consists of state errors and cost of input. It produces a nominal trajectory and nominal input as a result. However, the nominal model may not be an exact match of the actual plant due to modeling uncertainties. The errors may cause performance loss and even cause instability. So, the second part of the design is to introduce a feedback controller, which is also the tube of the MPC. The functionality of this tube is to compensate the error between the nominal position and real position. The tube minimizes the effects of disturbances due to modeling uncertainties and to make the actual plant trajectory bounded and centered by the nominal trajectory. Figure 8 shows the flowchart of a tube-based MPC. An analog/digital (A/D) converter is used before the MPC to convert the continuous states to discretized states, which are then used in MPC. And a zero-order-holder (ZOH) is used to convert the nominal states and inputs to continuous functionals, which match the feedback controller.

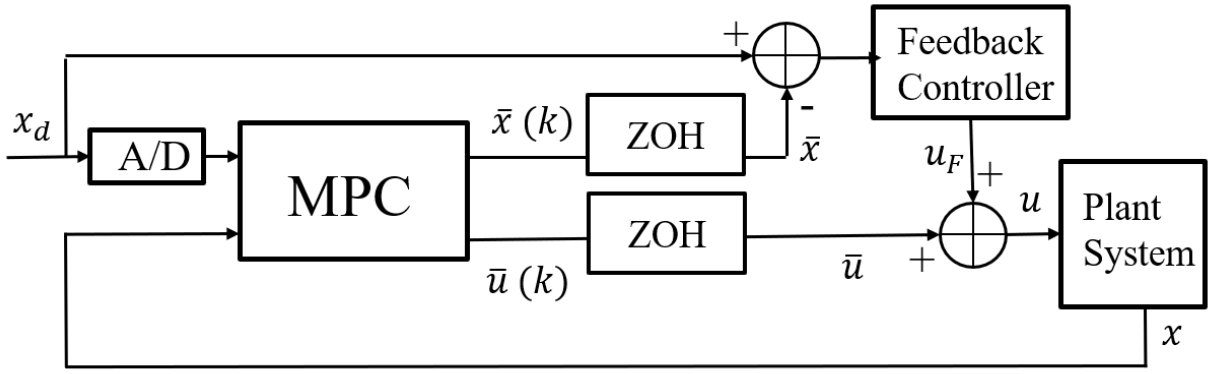

Figure 8 Block diagram of tube-based MPC

In this thesis, a gradient search based MPC [54] was used to compute nominal control input and the PD-type DSC controller is the feedback law.

4.2.1 Gradient Projection Dynamic Control Allocation

The optimal control problem is stated as

$$\begin{aligned} \min_{u(t)} \quad & J(x(k),\{\bar{u}\}_k) = V(\Delta\bar{x}(k+N)) + \sum_{m=k}^{m+N-1} l(\Delta\bar{x}(m),\Delta\bar{u}(m)) \\ \text{subject to:} \quad & \bar{x}(m+1) = g(\bar{x}(m),\bar{u}(m)) \\ & \bar{x} = x(k) \\ & \bar{u} \in \mathcal{U} \end{aligned} \tag{4.12}$$

According to the formulation, sampling time instance k satisfies $k \in \left[T_0, T_f\right]$, which is the time period of the control process. At k, constant prediction horizon of MPC is designed to be $\left[k, k+N-1\right]$, where N defines the prediction horizon length, and m is a time instance in the

prediction horizon. The cost function $J(x(k),\bar{u}) \in \mathbb{R}^+ \cup \{0\}$ at k is formed by the step cost function $l(\Delta\bar{x}(m),\Delta\bar{u}(m))$, and the terminal cost $V(\Delta\bar{x}(k+N))$. In the cost function $\Delta\bar{x} = x_d - \bar{x}$ where $x_d \in \mathbb{R}^3$ and $\bar{x} \in \mathbb{R}^3$ are the desired and nominal states, respectively and $\Delta\bar{u} = u_d - \bar{u}$ where $u_d \in \mathcal{U}$ and $\bar{u} \in \mathcal{U}$ are the desired and nominal inputs, respectively, and $\{\bar{u}\}_k = \{\bar{u}(m),\bar{u}(m+1),\ldots,\bar{u}(m+N-1)\}_k$ is the nominal input sequence over prediction horizon at time k. In this thesis, a quadratic cost function of the form

$$l\left(\Delta\bar{x}(m),\Delta\bar{u}(m)\right) = \Delta\bar{x}(m)^T Q\Delta\bar{x}(m) + \Delta\bar{u}(m)^T R\Delta\bar{u}(m)$$

$$\Delta\bar{x}(k+N)^T P\Delta\bar{x}(k+N),$$

where $P,Q \in \mathbb{R}^{3\times3}$ and $R \in \mathbb{R}^1$ are all PD and symmetric weight matrices so that l and V are PD and radially unbounded (RU).

Pontryagin's Minimum Principle states that optimal solution solved in the optimization problem satisfies all the conditions for the finite time horizon if it minimizes the Hamiltonian.

Given the definition of the optimal control problem in (4.17) the Hamiltonian is defined as

$$H(\bar{x},\lambda,\bar{u}) = l(\bar{x},\bar{u}) + \lambda^T g(\bar{x},\bar{u}) \tag{4.13}$$

where $\lambda \in \mathbb{R}^3$ is the co-state vector. After analytically solving for the gradient of the Hamiltonian a gradient-based iterative solver can be used to solve for $\{\bar{u}^*\}$ that minimizes the Hamiltonian and subsequently solves the optimal control problem in (4.17) over prediction horizon. To ensure that the control signals stay within the specified bounds a projection function can be used at each iteration, where the projection function can be defined as

$$\psi(\bar{u}) = \begin{cases} \bar{u}^-, & \bar{u} < \bar{u}^- \\ \bar{u}, & \bar{u}^- \le \bar{u} \le \bar{u}^+ \\ \bar{u}^+, & \bar{u}^+ < \bar{u} \end{cases}, \tag{4.14}$$

One iterative, gradient-based method that may be used for solving (4.17) is the gradient projection algorithm [30][55], which can be summarized as in Figure 9. In this algorithm, the early termination condition of the iterative solver forces the solver to stop if $j > M$ ($M \in \mathbb{I}^+$) where M is the maximum iteration limit. This ensures that the gradient projection algorithm can be implemented in real time by limiting the number of iterations at each time step. When the solver terminates due to exceeding the maximum iteration limit the solution is suboptimal.

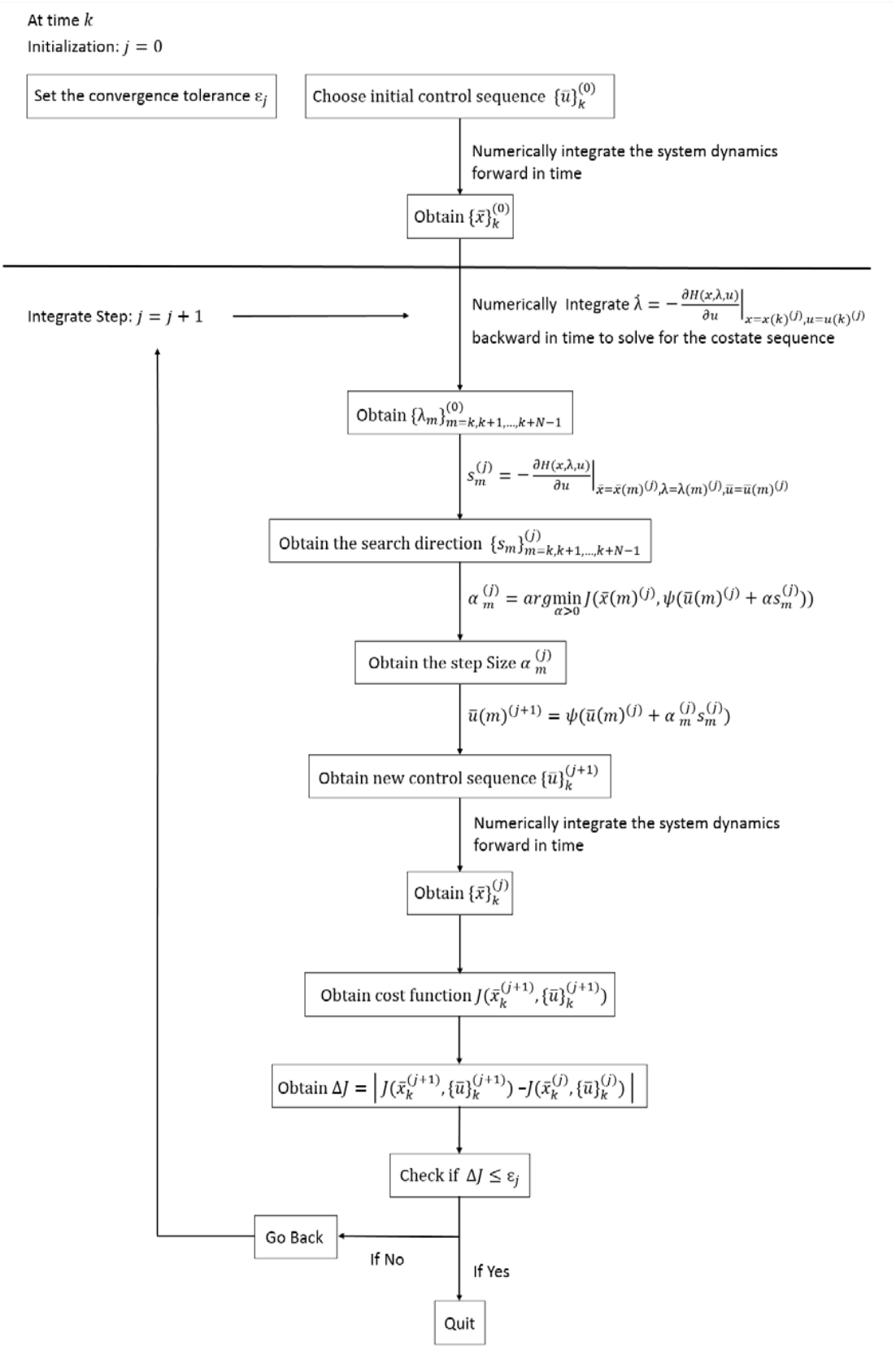

Figure 9 Nominal MPC algorithm

Assuming at time k the optimal control input sequence can be denoted as

$$\{\bar{u}^*\}_k = \{\bar{u}^*(m), \bar{u}^*(m+1), \ldots, \bar{u}^*(m+N-1)\}_k .$$

Afterwards, the first control input $u(k) = \bar{u}(m)^* \in \{\bar{u}^*\}_k$ is applied to the actual system. The corresponding optimal nominal state sequence and actual state sequence are defined to be $\{\bar{x}^*\}_k = \{\bar{x}^*(m), \bar{x}^*(m+1), \ldots, \bar{x}^*(m+N-1)\}$ and $\{x(k)\} = \{x(m), x(m+1), \ldots, x(m+N-1)\}$ respectively. Therefore, we can define the optimal cost at k to be

$$\sum_{m=k}^{m+N-1} l(\Delta x^*(m), \Delta u^*(m)) . \tag{4.15}$$

For the optimization problem (4.12), several assumptions can be made:

Assumption 4.1: The optimization problem in (4.17) has optimal solution, $\{u^*\}$, over MPC prediction horizon $\forall k$ and N.

Assumption 4.2: If $\{\bar{u}^*\}_k$ exists, there also exist a law $\kappa_N(x(k+1))$ that makes the sequence

$$\{\hat{u}\}_{k+1} = \{\bar{u}^*(m+1), \bar{u}^*(m+2), \ldots, \bar{u}^*(m+N-1), \kappa_N(x(k+1))\} \tag{4.16}$$

feasible for the optimization problem at time $k+1$. Therefore $\{\hat{u}\}_{k+1}$ is the initial input for the optimization problem over prediction horizon $[k+1, k+N]$.

Assumption 4.3: At $k \in [T_0, T_f]$, the following relation is satisfied.

$$V(\Delta\hat{x}(k+N+1)) - V(\Delta\bar{x}^*(k+N)) \le -l(\Delta\hat{x}(k+N), \Delta\hat{u}(k+1)), \tag{4.17}$$

where

$$\Delta\bar{x}^*(k+N) = x_d(k+N) - \bar{x}^*(k+N) ,$$

$$\Delta\hat{x}(k+N+1) = x_d(k+N+1) - g(\bar{x}^*(k+N), \kappa_N(x(k+1))),$$

and

$$\Delta\hat{u}(k+1) = u_d(k+1) - \kappa_N(x(k+1)).$$

According to Assumption 4.2, the initial cost at $k+1$ with the nominal dynamics can be written as

$$J(\bar{x}(k+1), \{\hat{u}\}_{k+1}) = V(\Delta\hat{x}(k+N+1)) + \sum_{m=k}^{m+N-1} l(\Delta\hat{x}(m), \Delta\hat{u}(m)).$$

By exploring system (3.7) we can notice that at the starting time in a prediction horizon

$$x(m+1) = g(\bar{x}(m), \bar{u}(m)) + w(m), \tag{4.18}$$

where $\bar{x}(m) = x(k)$, if it is at k. After the feedback control, which drives the actual position to the nominal one, i.e., diminish w, let's assume

$$x(m+1) = \bar{x}(m+1) + \zeta(m) = g(\bar{x}(m) + \zeta(m-1), \bar{u}(m)). \tag{4.19}$$

According to (4.19), cost at $k+1$ with the actual dynamics is

$$J(x(k+1), \{\hat{u}\}_{k+1}) = V(\Delta\hat{x}(k+N+1)) + \sum_{m=k}^{m+N-1} l(\Delta\hat{x}(m), \Delta\hat{u}(m)) + l_d, \tag{4.20}$$

where $l_d = l_d(x(k+1), \{\hat{u}\}_{k+1}, \{\zeta\}_{m=k,\ldots,m+N})$, and $\| l_d \| \leq \bar{l}_d$, is the disturbance to the cost function value, which affects the optimality.

To ensure stability of the MPC system some algorithms use a terminal constraint, but this can make the optimal control problem difficult and more time consuming to solve, so that make real time implementation of MPC even more challenging to accomplish. Instead of using a terminal constraint to stabilize the MPC the terminal cost function V, can be used as a control Lyapunov

function to ensure stability of the system. Assumption 4.3 is the key assumption to ensure the stability [28][45] and this assumption can be made approximately satisfied by solving the algebraic Riccati equation [30][55]

$$PA + A^T P - PBR^{-1}B^T P + Q = 0 \tag{4.21}$$

for the gain matrix P, where the matrices $A \in \mathbb{R}^{3\times 3}$ and $B \in \mathbb{R}^3$ are the linearized state-space dynamics of the nonlinear system. The dynamics can be linearized by using Jacobian linearization about the desired states and control signals (x_d and u_d, respectively) as

$$\begin{aligned} A &= \left.\frac{\partial f(x,u)}{dx}\right|_{x=x_d, u=u_d} \\ &= \begin{bmatrix} 0 & 1 & 0 \\ A_{21} & A_{22} & A_{23} \\ 0 & 0 & -\dfrac{1}{T_a} \end{bmatrix} \end{aligned}$$

$$\begin{aligned} B &= \left.\frac{\partial f(x,u)}{\partial u}\right|_{x=x_d,\ u=u_d} \\ &= \begin{bmatrix} 0 \\ 0 \\ 1 \end{bmatrix} . \end{aligned}$$

where

$$\begin{aligned} A_{21} = -\beta\cos(x_{1,d} + \theta_{eq}) - \alpha\Bigg[& d_1 + d_3 d_4 \mathrm{e}^{d_4(\frac{\pi}{2} - x_{1,d} - \theta_{eq})} \\ & - d_5 d_6 \mathrm{e}^{d_6(\frac{\pi}{2} - x_{1,d} - \theta_{eq})} + \left(2c_2\left(\frac{\pi}{2} - x_{1,d} - \theta_{eq}\right)c_1\right)\left(1 - c_3 x_{2,d}\right)x_{3,d}x_{4,d}\Bigg] \end{aligned} \tag{4.22}$$

$$A_{22} = -\alpha \left[d_2 + (c_2(\frac{\pi}{2} - x_{1,d} - \theta_{eq})^2 + c_1(\frac{\pi}{2} - x_{1,d} - \theta_{eq}) + c_0)c_3 x_{3,d} x_{4,d} \right],$$

$$A_{23} = \alpha \left[\left(c_2(\frac{\pi}{2} - x_{1,d} - \theta_{eq})^2 + c_1\left(\frac{\pi}{2} - x_{1,d} - \theta_{eq} \right) + c_0 \right)\left(1 - c_3 x_{2,d}\right) x_{4,d} \right],$$

and $x_{i,d}$ for $i = \{1, 2, 3\}$ is the i th element of x_d .

4.2.2 Feedback Controller

The feedback controller is designed to drive the actual state to the nominal state calculated by MPC. The error is defined as

$$e_1(t) = \bar{x}_1 - x_1,$$

where $\bar{x}_1$ is the nominal joint angle and x_1 is the actual joint angle.

The Lyapunov function of the nominal system under Lyapunov control law can be defined as:

$$V_{LK} \triangleq \frac{1}{2}e_1^2 + \frac{1}{2}e_2^2 + \frac{1}{2}e_{3dc}^2 + \frac{1}{2}e_3^2 + P. \tag{4.23}$$

The auxiliary error signal $e_2(t) \in \mathbb{R}$ is defined as $e_2 = \dot{e}_1 + \alpha_1 e_1$, $e_{3dc} \in \mathbb{R}$ and $e_3 \in \mathbb{R}$ are defined as

$$e_{3dc} = x_{3f} - x_3 - e_I, e_3 = \bar{x}_3 - x_{3f},$$

with actual muscle activation signal $x_3(t)$, nominal signal $\bar{x}_3(t)$, filtered desired signal $x_{3f}(t)$, which satisfies $\tau_3 \dot{x}_{3f} + x_{3f} = \bar{x}_3$ and a delay compensation term $e_I = \int_{t-\tau}^{t} u(\theta) d\theta$. $P \in \mathbb{R}^+$ is Lyapunov Krasovskii (LK) functionals, $P = \omega \int_{t-\tau}^{t} \left(\int_{s}^{t} \left\| \dot{u}(\theta) \right\|^2 d\theta \right) ds$, where $\omega \in \mathbb{R}^+$ is a subsequently defined control gain.

A similar proof can be seen in section 4.1.2.

4.2.3 Stability Analysis

MPC method computes the discrete optimal control sequence. Zero order holder (ZOH) was used to convert discrete signal from MPC to continuous signal, and the feedback controller also provides continuous control signal. The control signals from MPC and feedback controller are summed up and then be applied to the actual system.

After the feedback controller, the Lyapunov function can be proved bounded and the system is UUB.

$$V(t) \le V(0) e^{-\frac{\delta}{\lambda_2} t} + \frac{\nu \lambda_2}{\delta} \left(1 - e^{-\frac{\delta}{\lambda_2} t} \right) \tag{4.24}$$

So, the states error can be bounded by a small constant. If the nominal model can exactly represent the system, meaning the error between the nominal model and the system is zero, there would be no disturbance term $\bar{l}_d$ in the cost function of actual dynamics (4.20). In other words, this disturbance term can be represented by the states error.

The optimal step cost at step *k* is

$$l^*(\Delta \bar{x}(k), \Delta \bar{u}(k)) = \Delta \bar{x}^*(k)^T Q \Delta \bar{x}^*(k) + \Delta \bar{u}^*(k)^T R \Delta \bar{u}^*(k) \tag{4.25}$$

where $\Delta\bar{x}^* = \bar{x} - \bar{x}_d$ and $\Delta\bar{u}^* = \bar{u} - \bar{u}_d$ are states error and input error of the optimal solution calculated by MPC.

The disturbance cost at *k* is

$$l_d = l_d(x(k+1), \{\hat{u}\}_{k+1}, \{\zeta\}_{m=k,\ldots,m+N}) \le \bar{l}_d \tag{4.26}$$

where ζ is the source of the disturbance which is defined by $\zeta = x - \bar{x}$

Substitute (4.17) into (4.12) we can obtain

$$\begin{aligned} J(x(k+1), \{\hat{u}\}_{k+1}) - J(x^*(k), \{\bar{u}\}_k^*) &= V(\Delta\hat{x}(k+N+1)) - V(\Delta\bar{x}^*(k+N)) \\ &+ l(\Delta\hat{x}(k+N), \Delta\hat{u}(k+1)) - l^*(\Delta x(k), \Delta u(k)) + l_d \\ &\le -l^*(\Delta x(k), \Delta u(k)) + \bar{l}_d \\ &\le 0, \end{aligned} \tag{4.27}$$

Where $J(x^*(k), \{\bar{u}\}_k^*$ represents for the optimal cost in step k and $J(x(k+1), \{\hat{u}\}_{k+1})$ represents for the cost of the initial guess at step $k+1$. Even if it does not always hold, the increasing error would cause $l^*(\Delta x(k), \Delta u(k))$ to increase and finally makes $l^*(\Delta x(k), \Delta u(k)) \ge \bar{l}_d$

Therefore, the cost is bounded over time.

4.2.4 Simulation Results

The simulation problem is a regulation problem, which is to move the leg to a specific angle and to keep the knee angle still. The parameters of the model are obtained by system identification of subject with SCI, which are listed in Table 1. An uncertainty of input time delay is added to the plant to test the robustness of the controller. The diagonal weigh matrices are:

$$diag(Q) = [100, 5, 1];$$
$$R = 10$$

After adding a 100ms input time delay to make the mismatch between the model and the system, results can be shown in the following figures.

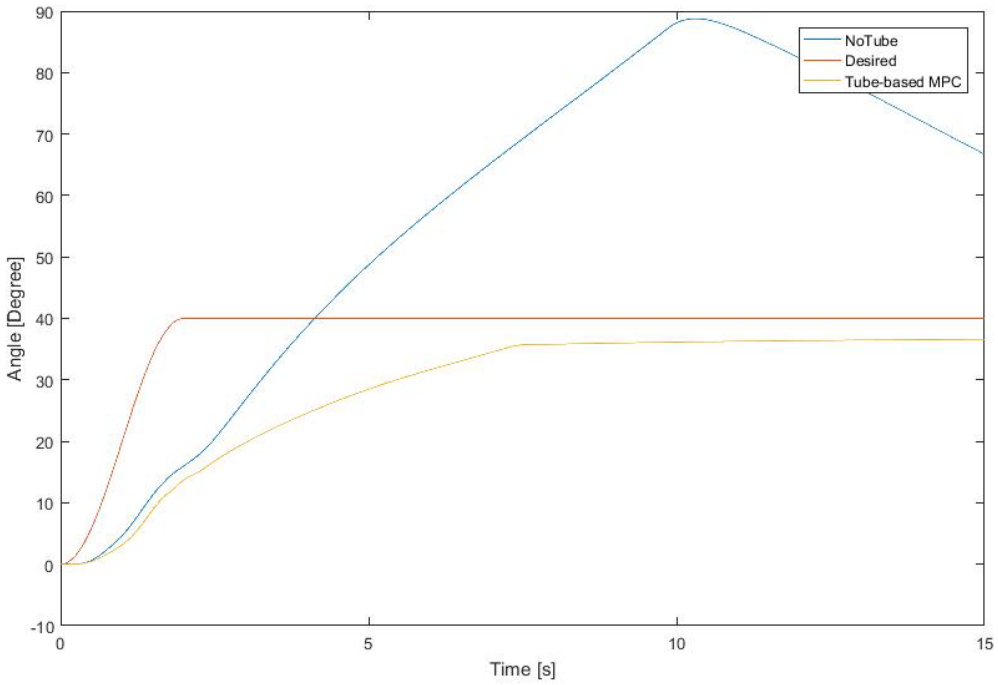

Figure 10 The output performance of nominal MPC (blue) and tube-based MPC (yellow), desired output is in red

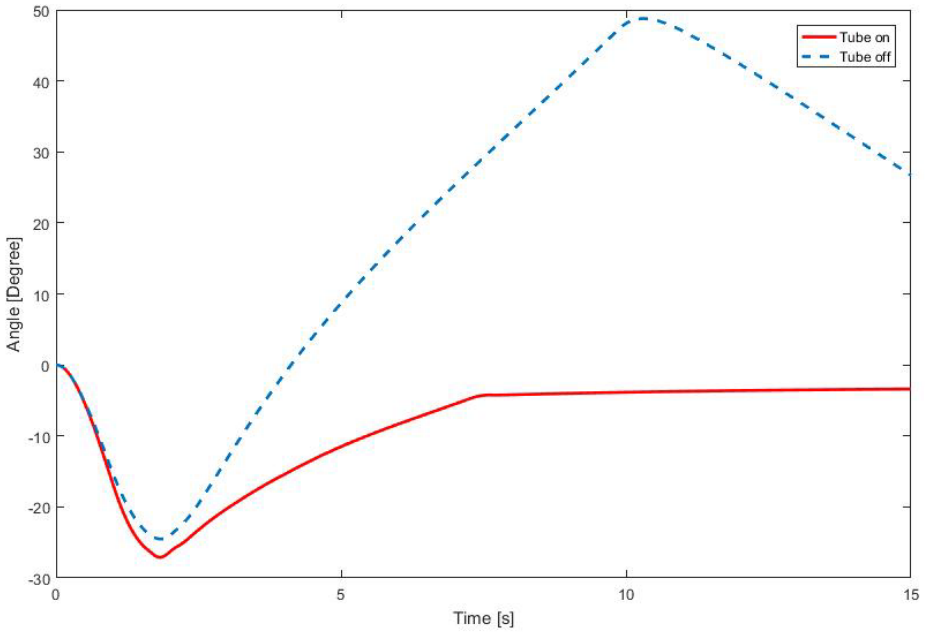

Figure 11 Output error of nominal MPC (dashed blue) and tube-based MPC (solid red)

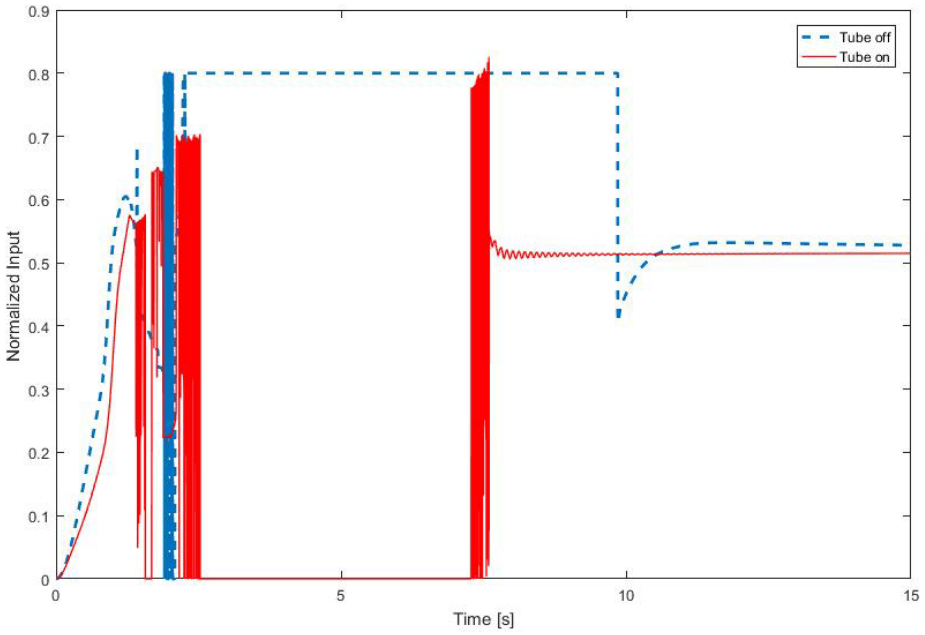

Figure 12 Normalized FES input of nominal MPC (dashed blue) and tube-based MPC (solid red)

The input time delay uncertainty was set to 100ms. From Figure 10, the pure nominal MPC cannot catch the change of the model. Because the model is different from the real plant, the actual output is different from the nominal output. And the error was cumulated with time, making the nominal output trajectory away from the desired angle. But after adding the tube, the error between the real output and nominal output is minimized so that the initial guess of the step $k+1$ is not far from the nominal sequence and the cumulated disturbance error is largely canceled. From Figure 10 and Figure 11, obvious improvement by the tube can be noticed. The error of two controllers can be found more explicitly from Figure 11. And normalized input effected by the tube is shown from Figure 12 .Through calculation of RMS value of input, $Urms, tube = 0.41$, $Urms, notube = 0.61$. The tube indeed reduced the input and saved energy.

4.2.5 Experimental Results

Tube-based MPC experiment was performed on an able-bodied subject. The parameter estimation for the subject are shown in Table 2. The parameters were obtained from system identification. During these experiments, the electrodes were placed on the quadriceps muscles and bipolar and 35 Hz pulse train with a pulse width of 400 microseconds was used. The system identification method can be referred to [15]. The parameters given in Table 2 are used in the model of the nominal MPC

Table 2 Estimated parameters of the subject C2

Parameter	Value	Parameter	Value
α	$1.32\frac{1}{kgm^2}$	d_6	-39.7865
β	$40.59\ \frac{1}{kgm^2}$	c_0	95.5618 Nm
θ_{eq}	0.35 radians	c_1	0.6055 Nm
d_1	2.29×10^{-14} Nm	c_2	0.6927 Nm
d_2	1.70 Nms	c_3	1.0949
d_3	1.64 Nm	T_a	0.27 seconds
d_4	1.60	I_t	21.21 mA
d_5	0.74 Nm	I_s	60.09 mA

The weight matrices in the integral cost function are selected as

$$diag(Q) = [50, 5, 1];$$
$$R = 10;$$

These weight matrices were selected by tuning them in the experiments until good results were achieved (gradually increase them until performance did not improve). And linearized matrices A and B are calculated by solving the Riccati Equation (4.21), which is a necessary condition for stability.

The gains of the tube, in other words, the DSC controller, are selected to be:

$$\alpha_1 = 15.0,\ \alpha_2 = 2.0,\ \text{k} = 3.0,\ \tau_3 = 0.02$$

These gains were obtained by tuning them without MPC until the real system output is regulated to an angle or at least bounded degree. Different trials were done to an able-bodied subject, one trial with the tube and in the other trial the gain of the tube is zero, meaning the tube is off. It has hypothesized that due to the difference between the nominal model and the real system dynamics, the tube-based MPC should work better than the nominal model MPC.

The experiments were performed on a leg extension machine as shown in Figure 13.

Figure 13 A subject sitting in a leg extension machine with surface electrodes on the quadricep muscles.

The results of experiments can be found from Figure 14 to Figure 22

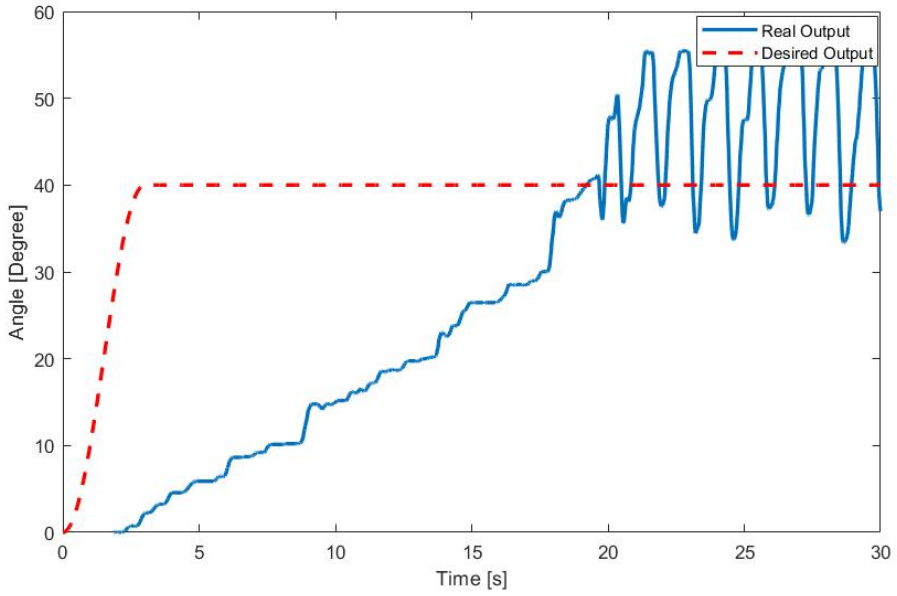

Figure 14 Output angle controlled by normalized MPC, no tube involved.

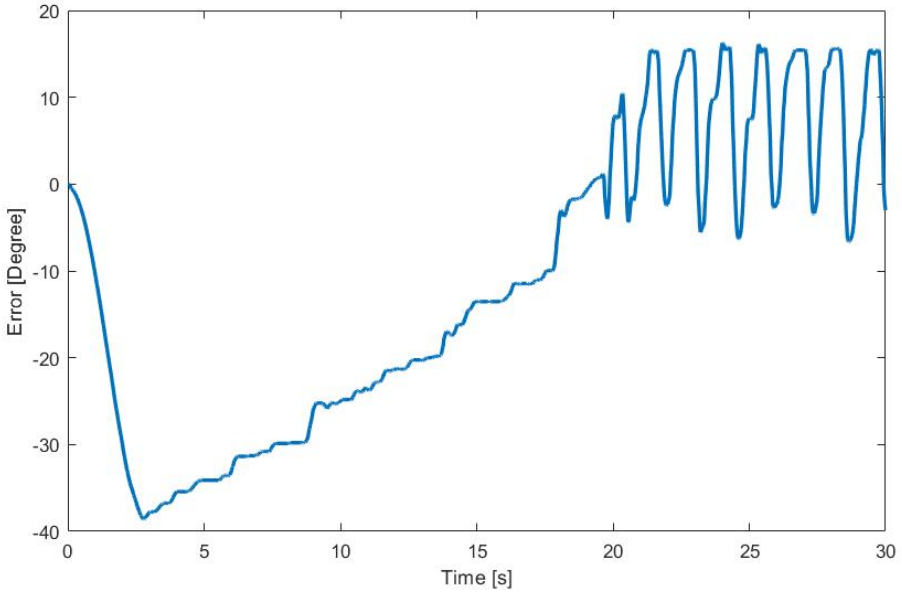

Figure 15 Output error controlled by the nominal MPC, no tube involved.

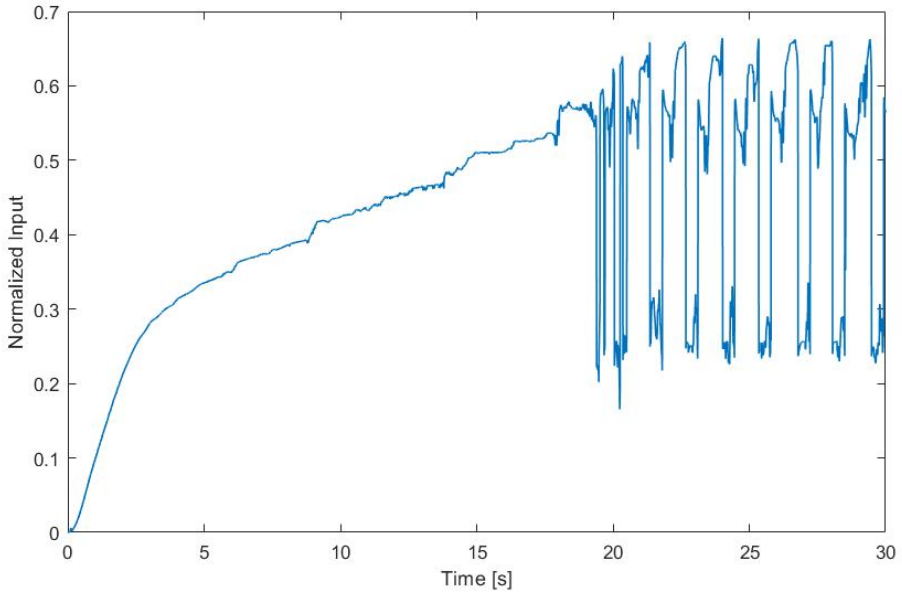

Figure 16 Normalized FES input calculated by nominal MPC, no tube involved

Figure 14 to Figure 16 illustrate the control performance of the nominal MPC which does not consider disturbances caused by EMD and the parameter estimation errors. Because the parameter estimation test is done prior to the real MPC test, the day-to-day variations are likely to creates mismatch between actual plant and the estimated model. The performance of the MPC controller with no tube was unsatisfactory. First, it did not follow the desired output trajectory and second, it did not keep the shank at a stabilized angle.

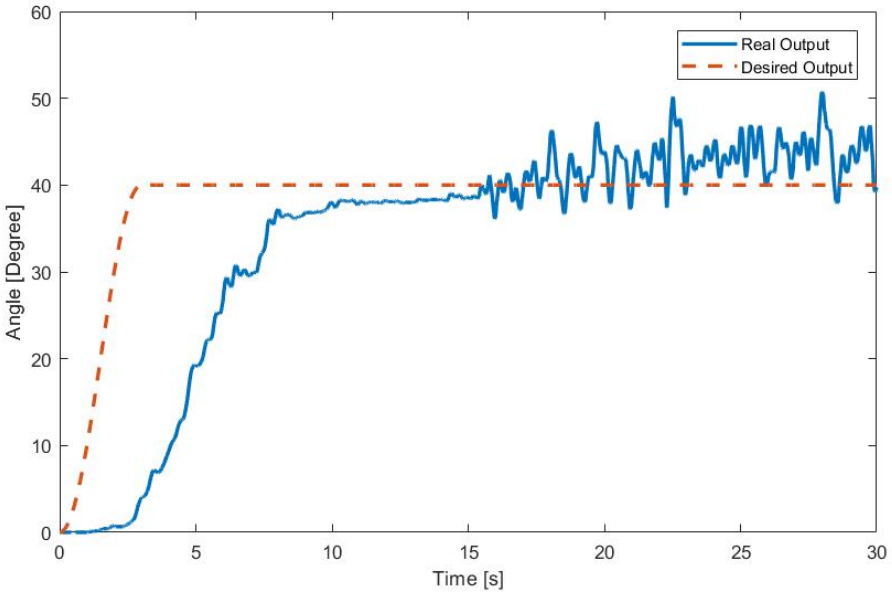

Figure 17 Output angle controlled by tube-based MPC, tube with a low gain (0.2) is involved.

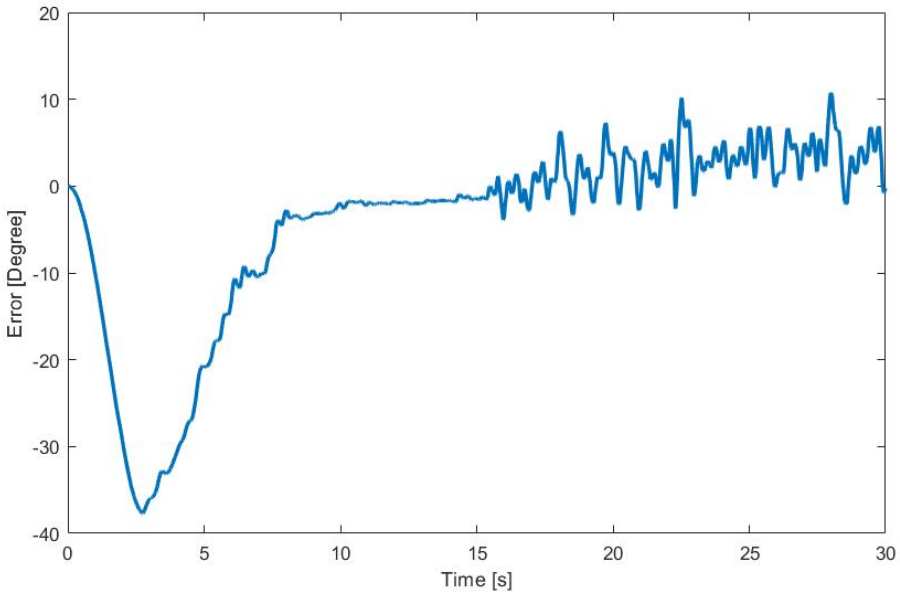

Figure 18 Output error controlled by tube-based MPC, tube with a low gain (0.2) is involved

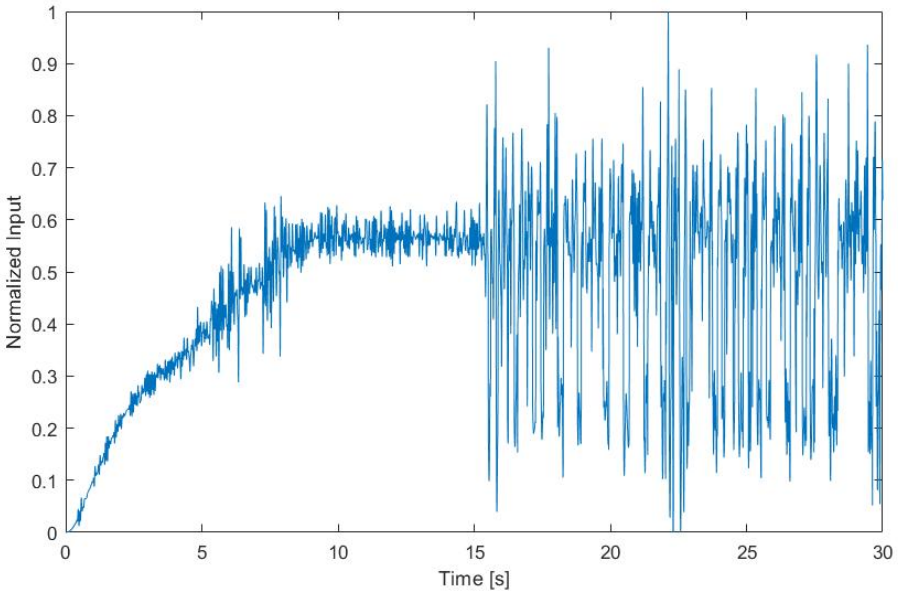

Figure 19 Normalized FES input controlled by tube-based MPC, tube with a low gain (0.2) is involved

Figure 17 to Figure 19 illustrate the control performance of a tube-based MPC. The gain of the tube output is chosen to be small at first and was increased gradually to see the influence of the tube. Though more oscillations are observed but they oscillate around a constant value. During the experiment, the subject felt smoother increase of stimulation and less oscillation after it reached the desired angle. The oscillations occur because the tube tries to correct the output of the nominal MPC, it obviously increases the accuracy of the output performance.

Figure 20 to Figure 22 illustrate the control performance of the tube-based MPC with a high output gain. As shown in Figure 20, by increasing the gain of the tube output, the oscillation becomes less, and the output behavior grows better.

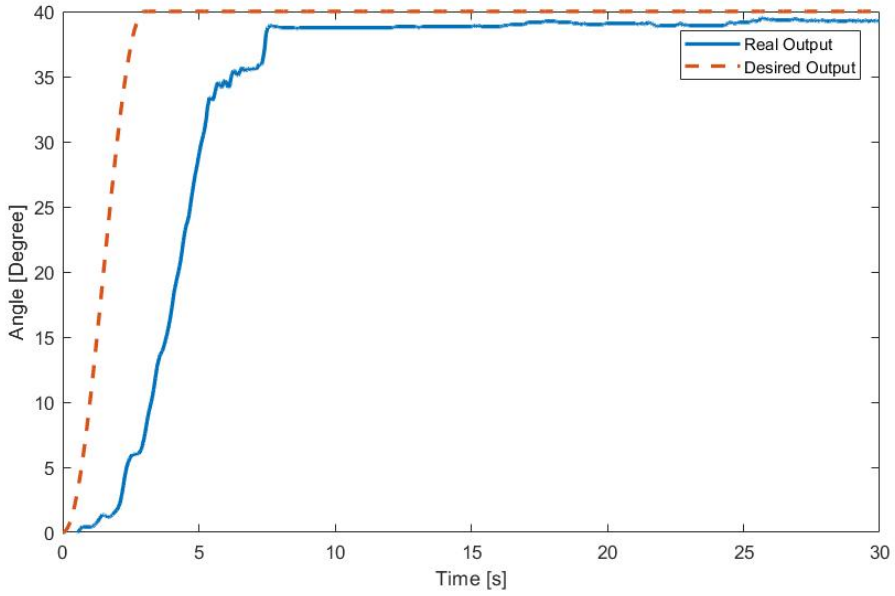

Figure 20 Output angle controlled by tube-based MPC, tube with a low gain (0.8) is involved.

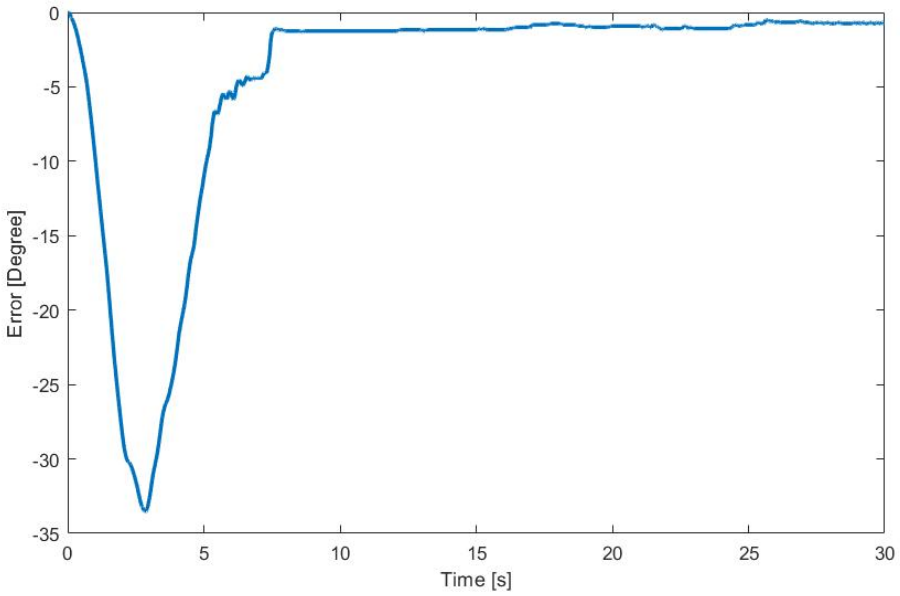

Figure 21 Output error controlled by tube-based MPC, tube with a low gain (0.8) is involved.

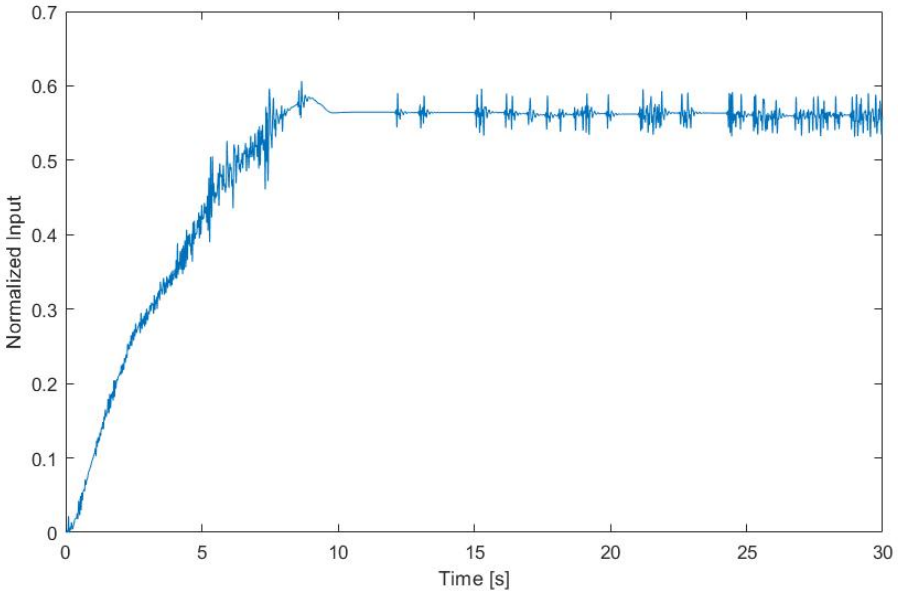

Figure 22 Normalized FES input controlled by tube-based MPC, tube with a low gain (0.8) is involved.

This controller compensates the disturbance of the system and can make the output behavior follow the desired output well. In this experimental session, the subject can follow the desired trajectory in the rising region, only a small lag is observed. When the shank reaches the desired position, the FES kept producing proper stimulations to hold the position. And this control result is the best of all three controllers. With the increase of tube gain, the performance improves.

5.0 CONCLUSION AND DISCUSSIONS

This thesis investigated two robust MPC methods, Lyapunov-based MPC and tube-based MPC, for controlling FES to obtain knee extension. The controller were motivated to address the issues of parametric uncertainties and EMD.

In the Lyapunov-based MPC method, the contractive constraint is proven to be able to ensure the control input remains in the feasible region. The simulation results were obtained by minimizing a cost function via interior point method. The results show that this method can guarantee the performance of the controller. The Lyapunov-based MPC seeks for optimal solutions within the stability region reconfigured by a feedback law. Therefore, the stability is achieved automatically. In addition, for a nonlinear system finding the global optimum cannot be guaranteed, it is like to add a perturbation to the Lyapunov control and choosing the control trajectory that gives the lower cost. In the Lyapunov-based MPC, a nominal model is used by the MPC and to generate Lyapunov constraints. This makes the Lyapunov-based MPC not robust to system disturbances, such as due to parameter estimation errors.

Tube-based MPC is more robust to Lyapunov-based MPC because the disturbance errors can be compensated by the feedback controller. In the tube-based MPC, the robustness is improved by using a tube centered by the nominal state sequence. When the difference between the nominal model and the plant exists, i.e. the nominal model cannot represent the plant well, the nominal MPC itself is not adequate to stabilize the system. The existence of the tube can drive the actual

state back to the nominal ones, making the nominal MPC work correctly. The stability of the tube-based MPC largely depends on the performance of the tube or the feedback controller.

Gradient -based search is used to solve for the minimum of the cost function so the computation speed is relatively fast and the tube-based MPC can be applied in real time. The experimental results showed that the tube-based MPC can be applied to control FES that elicits leg extension and regulate the knee at a desired angle. Future efforts will be to extend the tube-based MPC for knee tracking control.

BIBLIOGRAPHY

[1] NSCISC National Spinal Cord Injury Statistical Center, Annual Report, 2016

[2] Peckham PH, Keith MW, Kilgore KL, Grill JH, Wuolle KS, Thrope GB, Gorman P, Hobby J, Mulcahey MJ, Carroll S, Hentz VR. Efficacy of an implanted neuroprosthesis for restoring hand grasp in tetraplegia: a multicenter study. *Archives of physical medicine and rehabilitation*. 2001 Oct 31;82(10):1380-8.

[3] Wiesener C, Schauer T. The Cybathlon-RehaBike: Inertial-Sensor-Driven Functional Electrical Stimulation Cycling by Team Hasomed. *IEEE Robotics & Automation Magazine*. 2017 Nov 10.

[4] Sharma N, Dani A. Nonlinear estimation of gait kinematics during functional electrical stimulation and orthosis-based walking. In *American Control Conference (ACC)*, 2014 2014 Jun 4 (pp. 4778-4783). *IEEE*.

[5] Kirsch N, Alibeji N, Dicianno BE, Sharma N. Switching control of functional electrical stimulation and motor assist for muscle fatigue compensation. In *American Control Conference (ACC)*, 2016 2016 Jul 6 (pp. 4865-4870). *IEEE*.

[6] Kobetic R, Triolo RJ, Uhlir JP, Bieri C, Wibowo M, Polando G, Marsolais EB, Davis JA, Ferguson KA, Sharma M. Implanted functional electrical stimulation system for mobility in paraplegia: a follow-up case report. *IEEE Transactions on Rehabilitation Engineering*. 1999 Dec;7(4):390-8.

[7] Sharma N, Stein R. Gait planning and double support phase model for functional electrical stimulation-based walking. In *Engineering in Medicine and Biology Society (EMBC)*, 2012 *Annual International Conference of the IEEE* 2012 Aug 28 (pp. 1904-1907). IEEE.

[8] Ha KH, Murray SA, Goldfarb M. An approach for the cooperative control of FES with a powered exoskeleton during level walking for persons with paraplegia. *IEEE Transactions on Neural Systems and Rehabilitation Engineering*. 2016 Apr;24(4):455-66.

[9] Paillard T, Lafont C, Pérès C, Costes-Salon MC, Soulat JM, Montoya R, Dupui P. Is electrical stimulation with voluntary muscle contraction of physiologic interest in aging women?. In *Annales de readaptation et de medecine physique: revue scientifique de la Societe francaise de reeducation fonctionnelle de readaptation et de medecine physique* 2005 Feb (Vol. 48, No. 1, pp. 20-28).

[10] Bajd T, Kralj A, Turk R. Standing-up of a healthy subject and a paraplegic patient. *Journal of biomechanics.* 1982 Jan 1;15(1):1-0.

[11] Hoshimiya N, Naito A, Yajima M, Handa Y. A multichannel FES system for the restoration of motor functions in high spinal cord injury patients: a respiration-controlled system for multijoint upper extremity. *IEEE Transactions on Biomedical Engineering*. 1989 Jul;36(7):754-60.

[12] Kralj AR, Bajd T. *Functional electrical stimulation: standing and walking after spinal cord injury.* CRC press; 1989 Jan 31.

[13] Lynch CL, Popovic MR. Functional electrical stimulation. *IEEE control systems*. 2008 Apr;28(2):40-50.

[14] Alibeji N, Kirsch N, Farrokhi S, Sharma N. Further results on predictor-based control of neuromuscular electrical stimulation. *IEEE Transactions on Neural Systems and Rehabilitation Engineering*. 2015 Nov;23(6):1095-105.

[15] Kirsch N, Alibeji N, Sharma N. Nonlinear model predictive control of functional electrical stimulation. *Control Engineering Practice*. 2017 Jan 31;58:319-31.

[16] Dreibati B, Lavet C, Pinti A, Poumarat G. Influence of electrical stimulation frequency on skeletal muscle force and fatigue. *Annals of physical and rehabilitation medicine.* 2010 May 31;53(4):266-77.

[17] Ajoudani A, Erfanian A. A neuro-sliding-mode control with adaptive modeling of uncertainty for control of movement in paralyzed limbs using functional electrical stimulation. *IEEE Transactions on Biomedical Engineering*. 2009 Jul;56(7):1771-80.

[18] Sharma N, Gregory CM, Dixon WE. Predictor-based compensation for electromechanical delay during neuromuscular electrical stimulation. *IEEE Transactions on Neural Systems and Rehabilitation Engineering*. 2011 Dec;19(6):601-11.

[19] Hunt KJ, Stone B, Negard NO, Schauer T, Fraser MH, Cathcart AJ, Ferrario C, Ward SA, Grant S. Control strategies for integration of electric motor assist and functional electrical stimulation in paraplegic cycling: utility for exercise testing and mobile cycling. *IEEE Transactions on Neural systems and rehabilitation engineering*. 2004 Mar;12(1):89-101.

[20] Alibeji N, Kirsch N, Sharma N. Dynamic surface control of neuromuscular electrical stimulation of a musculoskeletal system with activation dynamics and an input delay. In *American Control Conference (ACC)*, 2015 2015 Jul 1 (pp. 631-636). IEEE.

[21] Mhaskar, P, El-Farra, NH and Christofides, PD, 2005. Predictive control of switched nonlinear systems with scheduled mode transitions. *IEEE Transactions on Automatic Control*, 50(11), pp.1670-1680.

[22] Esfanjani RM, Towhidkhah F. Application of nonlinear model predictive controller for FES-assisted standing up in paraplegia. In *Engineering in Medicine and Biology Society*, 2005. *IEEE-EMBS* 2005. 27th *Annual International Conference* of the 2006 Jan 17 (pp. 6210-6213). IEEE.

[23] Liu J, Muñoz de la Peña D, Christofides PD, Davis JF. Lyapunov-based model predictive control of nonlinear systems subject to time-varying measurement delays. *International Journal of Adaptive Control and Signal Processing*. 2009 Aug 1;23(8):788-807.

[24] Michalska H, Mayne DQ. Receding horizon control of nonlinear systems. InDecision and Control, 1989., *Proceedings of the 28th IEEE Conference* on 1989 Dec 13 (pp. 107-108). IEEE.

[25] Diehl M, Findeisen R, Allgöwer F, Bock HG, Schlöder JP. Nominal stability of real-time iteration scheme for nonlinear model predictive control. *IEEE Proceedings-Control Theory and Applications*. 2005 May 1;152(3):296-308.

[26] Lee JH, Cooley B. Recent advances in model predictive control and other related areas. In *AIChE Symposium Series* 1997 (Vol. 93, No. 316, pp. 201-216). New York, NY: American Institute of Chemical Engineers, 1971-c2002.

[27] Wikipedia contributors. "Model predictive control." Wikipedia, The Free Encyclopedia. Wikipedia, The Free Encyclopedia, 22 Nov. 2017. Web. 23 Nov. 2017.

[28] Mayne DQ, Rawlings JB, Rao CV, Scokaert PO. Constrained model predictive control: Stability and optimality. *Automatica*. 2000 Jun 30;36(6):789-814.

[29] Mayne DQ, Seron MM, Raković SV. Robust model predictive control of constrained linear systems with bounded disturbances. *Automatica*. 2005 Feb 28;41(2):219-24.

[30] Graichen K, Käpernick B. A real-time gradient method for nonlinear model predictive control. In *Frontiers of Model Predictive Control* 2012. In Tech.

[31] Mayne DQ, Kerrigan EC, Van Wyk EJ, Falugi P. Tube-based robust nonlinear model predictive control. *International Journal of Robust and Nonlinear Control.* 2011 Jul 25;21(11):1341-53.

[32] Kirsch NA, Alibeji NA, Sharma N. Model predictive control-based dynamic control allocation in a hybrid neuroprosthesis. In *ASME 2014 Dynamic Systems and Control Conference* 2014 Oct 22 (pp. V003T43A003-V003T43A003). American Society of Mechanical Engineers.

[33] Campo, Peter J., and Manfred Morari. "Robust model predictive control." *American Control Conference*, 1987. IEEE, 1987.

[34] Garcia CE, Prett DM, Morari M. Model predictive control: theory and practice—a survey. *Automatica*. 1989 May 1;25(3):335-48.

[35] Mahmood M, Mhaskar P. Lyapunov-based model predictive control of stochastic nonlinear systems. *Automatica*. 2012 Sep 30;48(9):2271-6.

[36] Christofides PD, Liu J, De La Pena DM. Conclusions. In *Networked and Distributed Predictive Control* 2011 (pp. 219-220). Springer London.

[37] de Oliveira Kothare SL, Morari M. Contractive model predictive control for constrained nonlinear systems. *IEEE Transactions on Automatic Control*. 2000 Jun;45(6):1053-71.

[38] Mhaskar P, El-Farra NH, Christofides PD. Stabilization of nonlinear systems with state and control constraints using Lyapunov-based predictive control. *Systems & Control Letters*. 2006 Aug 31;55(8):650-9.

[39] Ellis M, Christofides PD. Handling computational delay in economic model predictive control of nonlinear process systems. In *American Control Conference (ACC),* 2015 Jul 1 (pp. 2962-2967). IEEE.

[40] Ellis M, Christofides PD. On closed-loop economic performance under Lyapunov-based economic model predictive control. In *American Control Conference (ACC),* 2016 2016 Jul 6 (pp. 1778-1783). IEEE.

[41] Esfanjani RM, Reble M, Münz U, Nikravesh SK, Allgöwer F. Model predictive control of constrained nonlinear time-delay systems. In *Decision and Control, 2009 held jointly with the 2009 28th Chinese Control Conference. CDC/CCC 2009. Proceedings of the 48th IEEE Conference on* 2009 Dec 15 (pp. 1324-1329). IEEE.

[42] de la Pena DM, Christofides PD. Lyapunov-based model predictive control of nonlinear systems subject to data losses. *IEEE Transactions on Automatic Control*. 2008 Oct;53(9):2076-89.

[43] Liu J, Muñoz de la Peña D, Christofides PD, Davis JF. Lyapunov‐based Model Predictive Control of Particulate Processes Subject to Asynchronous Measurements. *Particle & Particle Systems Characterization.* 2008 Nov 1;25(4):360-75.

[44] Mayne DQ, Raković SV, Findeisen R, Allgöwer F. Robust output feedback model predictive control of constrained linear systems. *Automatica*. 2006 Jul 31;42(7):1217-22.

[45] Mayne DQ, Kerrigan EC. Tube-based robust nonlinear model predictive control. *IFAC Proceedings Volumes.* 2007 Dec 31;40(12):36-41.

[46] Farina M, Scattolini R. Tube-based robust sampled-data MPC for linear continuous-time systems. *Automatica*. 2012 Jul 31;48(7):1473-6.

[47] Lacourpaille L, Nordez A, Hug F. Influence of stimulus intensity on electromechanical delay and its mechanisms. *Journal of Electromyography and Kinesiology.* 2013 Feb 28;23(1):51-5.

[48] Linford CW, Hopkins JT, Schulthies SS, Freland B, Draper DO, Hunter I. Effects of neuromuscular training on the reaction time and electromechanical delay of the peroneus longus muscle. *Archives of physical medicine and rehabilitation.* 2006 Mar 31;87(3):395-401.

[49] Rushton DN. Functional electrical stimulation. *Physiological measurement*. 1997 Nov;18(4):241.

[50] Lin Y, Sontag ED. A universal formula for stabilization with bounded controls. *Systems & Control Letters*. 1991 Jun 1;16(6):393-7.

[51] Widjaja F, Shee CY, Au WL, Poignet P, Ang WT. Using electromechanical delay for real-time anti-phase tremor attenuation system using functional electrical stimulation. In *Robotics and Automation (ICRA), 2011 IEEE International Conference* on 2011 May 9 (pp. 3694-3699). IEEE.

[52] Sharma N, Gregory CM, Dixon WE. Predictor-based compensation for electromechanical delay during neuromuscular electrical stimulation. *IEEE Transactions on Neural Systems and Rehabilitation Engineering*. 2011 Dec;19(6):601-11.

[53] Alibeji N, Kirsch N, Dicianno BE, Sharma N. A Modified Dynamic Surface Controller for Delayed Neuromuscular Electrical Stimulation. *IEEE/ASME Transactions on Mechatronics*. 2017 Aug;22(4):1755-64.

[54] Kapernick B, Graichen K. The gradient based nonlinear model predictive control software GRAMPC. In *Control Conference (ECC), 2014 European* 2014 Jun 24 (pp. 1170-1175). IEEE.

[55] Graichen K, Kugi **A**. Stability and incremental improvement of suboptimal MPC without terminal constraints. *IEEE Transactions on Automatic Control.* 2010 Nov;55(11):2576-80.